lead us to speculate that synovial tissues contain multipotent cells with chondrogenic potential that might be involved in the repair process of articular cartilage defects and therefore might provide a good source for engineering articular cartilage.

There is accumulating evidence that TGF-β superfamily cytokines play an essential role in bone and cartilage development. Wozney and coworkers (19) reported that bone morphogenetic proteins (BMPs) induce early cartilage formation, and various studies have shown that TGF-β induces chondrocytic differentiation of undifferentiated mesenchymal cells (20–22). In the present study, we analyzed the role of TGF-β/BMP signaling on chondrogenic differentiation of human SFs by using the adenovirus vector-mediated gene transduction system. The introduction of an activated mutant of ALK3 (constitutively active activin receptor-like kinase 3 [ALK3^{CA}]), also known as BMP type IA receptor, induced chondrocyte-specific marker expression in the cells. ALK3 signaling involves two different downstream cascades, the Smad pathway and the p38 MAP kinase pathway. We used a combination of adenoviral gene delivery and chemical inhibition to analyze the role of these two signaling cascades in inducing differentiation of SF cells toward a chondrocyte phenotype and found that both pathways are essential for chondrogenic differentiation. Interestingly, activation of p38 pathways alone induced markers of terminal chondrocyte differentiation, type X collagen expression and mineralization, which was suppressed by Smad1 coexpression. These results suggest that both the Smad and p38 pathways are necessary for chondrogenic differentiation of SFs and that the balance between these two pathways determines the stage of differentiation.

Methods

Chemicals and antibodies. Alpha-modified minimum essential medium (α-MEM) was purchased from Gibco BRL, Life Technologies Inc. (Rockville, Maryland, USA), and fetal bovine serum (FBS), from Sigma-Aldrich (St. Louis, Missouri, USA). Anti-p38 MAPK and anti-phospho-p38 MAPK (Thr180/Tyr182) were obtained from Cell Signaling Inc. (Cummings Center, Beverly, Massachusetts, USA). Anti-Flag was purchased from Sigma-Aldrich, and anti-hemagglutinin (anti-HA) was from Santa Cruz Biotechnology Inc. (Santa Cruz, California, USA). Anti-phospho-Smad1/5/8, which recognizes the phosphorylated form of Smad1, Smad 5, and Smad8, and anti-phospho-Smad2 were from Cell Signaling Inc. Anti-type II collagen was purchased from Oncogen (Boston, Massachusetts, USA) and anti-type X collagen was from LSL Co. (Cosmo Bio, Tokyo, Japan). Other chemicals and reagents used in this study were of analytical grade.

Isolation of SFs from human synovial tissues. Synovial cells were obtained as previously described (13, 23, 24). In brief, with enzymatic digestion, human synovial cells were isolated from synovial tissues of the knee joints of ten rheumatoid arthritis patients (37–75 years of age; mean, 60.3 years of age) at the time of total knee arthroplasty operations. Written informed consent for subsequent experiments was obtained from each patient. Cells were suspended in α-MEM containing 10% FBS and were cultured in monolayers. After three to five passages, subcultured cells were composed of morphologically uniform fibroblastic cells (SFs) that were free of macrophages. They were infected with adenovirus vectors and cultured in pellets ("pellet culture"). Primary chondrocytes were obtained from articular cartilage resected during the surgeries. Cartilage was minced finely in phosphate-buffered saline (PBS), and chondrocytes were isolated by sequential digestion at 37°C with

0.25% (weight/volume) trypsin for 30 minutes and with 2 mg/ml of clostridial collagenase in α-MEM containing 10% FBS and antibiotics (penicillin at 100 µg/ml and streptomycin at 100 µg/ml) overnight on an orbital shaker. Cells were isolated by centrifugation and were resuspended in α-MEM with 10% FBS. Cells were cultured in monolayers for 1 day and then subjected to RNA isolation.

Constructs and gene transduction. The recombinant adenovirus vectors carrying various molecules that modulate TGF-β superfamily signaling pathways, that is, HA-tagged constitutively active TGF-β/BMP type I receptors (ALK3^{CA}, ALK5^{CA}, and ALK6^{CA}), constitutively active MKK6 (MKK6^{CA}), Flag-tagged Smad1 and Smad6 with CAG [cytomegalovirus IE enhancer + chicken β-actin promoter + rabbit β-globin poly(A) signal] promoter, were generated by the DNA-terminal protein complex method (25–27). SFs were infected with adenovirus vectors following a method previously described (13). In short, subconfluent SFs were incubated with a small amount of medium (α-MEM without serum) that contained the recombinant adenoviruses for 2 hours at 37°C at the indicated multiplicity of infection (MOI) and then with 10 times more medium to which 10% FBS had been added. Infected cells were cultured for additional 3 days for assessment of chondrogenic gene expression or were subjected to pellet culture 24 hours after the infection for histological examination.

Pellet cultures of isolated SFs. After 24 hours of viral infection, adherent cells were trypsinized and cells numbers were ascertained. Aliquots of 5 × 10^5 cells were spun down at 500 g in 15-ml polypropylene conical tubes in 5 ml of α-MEM with ascorbate 2-phosphate (0.1 mM) and 10% FBS. The cells were incubated at 37°C in 5% CO$_2$. Within 24 hours after incubation, the cells formed a single, free-floating pellet. The medium was changed every 2–3 days, and duplicate pellets were harvested after 3 and 7 days for real-time-PCR and Northern blotting and after 3 and 5 weeks for histological and immunohistochemical analysis. For visualization of the chondrogenic differentiation in vivo pellets were transplanted subcutaneously into *nu/nu* BALB mice (nude mice) after 3 days of pellet culture. Mice were sacrificed 5 weeks after transplantation and the pellets were recovered and subjected to toluidine blue staining as well as immunostaining with anti-type II collagen.

Immunoblotting. All the extraction procedures were performed at 4°C or on ice. Cells were washed with PBS and then lysed by the addition of TNE buffer (1% NP-40, 10 mM Tris-HCl, pH 7.8, 150 mM NaCl, 1 mM EDTA, 2 mM Na$_3$VO$_4$, 10 mM NaF, and 10 µg/ml aprotinin). Lysates were prepared by centrifugation at 10,000 g for 20 minutes. An equal amount (15 µg) of proteins was separated by electrophoresis on 10% SDS-polyacrylamide gels. After electrophoresis, proteins were electronically transferred onto a nitrocellulose membrane. Immunoblotting with specific antibodies was performed with ECL Western blotting reagents (Amersham Co., Arlington Heights, Illinois, USA) according to the conditions recommended by the supplier.

Histology and immunostaining. Pellet cultures were fixed with 3.7% formaldehyde, embedded in paraffin, and cut into sections 4 µm in thickness. Representative sections were subjected to Alcian blue staining, Alizarin red staining, and immunohistochemistry. Alcian blue staining was performed according to the protocol described previously (28). Briefly, after deparaffinization, sections were stained with 0.5% Alcian blue 8GX (Wako, Osaka, Japan) in 0.1 N HCl for 1 hour. Mineralization was assessed by Alizarin red staining. In brief, sections were immersed in Alizarin red solution (40 mM, at pH 4.0) for 8 minutes at room temperature, and nonspecific staining was removed by several washes in distilled water. For immunostaining with anti-type

II collagen or anti-type X collagen, we utilized a CSA Kit (DAKO, Carpinteria, California, USA) following the manufacturer's protocol.

Total RNA extraction and real-time PCR. Total RNA was isolated from SFs with ISOGEN (Wako) following the supplier's protocol. Complementary DNA (cDNA) was synthesized from 1 μg of total RNA with the Superscript II reverse transcriptase kit (Invitrogen, Carlsbad, California, USA). For real-time PCR, the ABI Prism Sequence Detection System 7000 was used. Primers were designed based on sequences obtained from GenBank and amplicons of 50–250 base pairs with a melting temperature of between 55°C and 60°C were selected. Aliquots of first-strand cDNA (1 μg) were amplified with the QuantiTect SYBER Green PCR Kit (Qiagen, Valencia, California, USA) under the following conditions: initial denaturation for 10 minutes at 94°C followed by 40 cycles consisting of 15 seconds at 94°C and 1 minute at 60°C. Data analysis consisted of fold induction, and the expression ratio was calculated from the differences in threshold cycles at which an increase in reporter fluorescence above a baseline signal could first be detected among three samples and was averaged for duplicate experiments. The primers we utilized in real-time PCR to detect sox9, type II collagen, type X collagen, osteocalcin, osteopontin, and GAPDH were as follows: sox9, 5'-AGAAG-GACCACCCGGATTAC-3' and 5'-AAGTCGATAGGGGGCTGTCT-3'; type II collagen, 5'-GGTGGCTTCCATTTCAGCTA-3' and 5'-TACCGGTATGTTTCGTGCAG-3'; type X collagen, 5'-AGGAAT-GCCTGTGTCTGCTT-3' and 5'-ACAGGCCTACCCAAACATGA-3'; osteocalcin, 5'-GTGCAGAGTCCAGCAAAGGT-3' and 5'-CGATAG-GCCTCCTGAAAGC-3'; osteopontin, 5'-ACAGCCAGGACTC-CATTGAC-3' and 5'-ACACTATCACCTCGGCCATC-3'; and GAPDH, 5'-GAAGGTGAAGGTCGGAGTCA-3' and 5'-GAAGATG-GTGATGGGATTTC-3'.

Northern blotting. Equal amounts (15 μg) of RNA were denatured in formaldehyde, separated by 1% agarose gel electrophoresis and transferred to a nitrocellulose membrane (Hybond N⁺) (Amersham Pharmacia, Piscataway, New Jersey, USA), followed by ultraviolet crosslinking. ULTRAHyb hybridization solution (Ambion, Austin, Texas, USA) was used according to the manufacturer's protocol. The blots were hybridized with a cDNA probe labeled with [α-^{32}P]dCTP using Ready-To-Go DNA Labeling Beads (Amersham Pharmacia). Rabbit type II collagen and aggrecan probes were generously provided by Yoshiyasu Iwamoto (Thomas Jefferson University, Philadelphia, Pennsylvania, USA). Membranes were washed in 2× SSC for 15 minutes at 42°C and then in 0.1× SSC for 30 minutes at 65°C. For visualization, X-ray film was exposed to membranes overnight at −80°C.

Osteoarthritis model mice. Osteoarthritic changes were developed in the knee joint by transection of the anterior cruciate ligament (ACL) and medial meniscus (MM) in C57BL/6 mice (mean age, 8 weeks) (29, 30). Briefly, after mice were anesthetized with ketamine and xylazine, a medial parapatellar skin incision was made. The subcutaneous tissues were incised and retracted, along with the articular capsule. The medial compartment of the knee joint was visualized and the ACL and MM were transected with a scalpel, and thereafter the capsule, medial retinaculum, and skin were sutured. Mice were housed in regular individual cages and allowed to exercise. Eight weeks after the surgery, the mice were sacrificed and paraffin-embedded sections of the affected joints were immunostained with anti-type X collagen and anti-phospho-p38 (Cell Signaling Technology Inc).

Results

Adenovirus-mediated gene transduction modulates the Smad and p38 pathways in SFs. We previously reported that adenovirus vectors can effi-

ciently transduce foreign genes into synovial cells both in vitro and in vivo and that adenovirus infection itself does not affect the phenotypes of the cells (13). We constructed adenovirus vectors to analyze the role of ALK signaling as well as the Smad pathways and p38 pathways, which lie downstream of ALK signaling. SFs were infected with adenovirus vectors carrying various signaling molecules that modulate TGF-β superfamily signaling pathways, that is, HA-tagged constitutively active ALK3, ALK5, and ALK6 constitutively active MKK6, and Flag-tagged Smad1 and Smad6, as well as a control virus carrying the β-galactosidase gene (LacZ virus), and gene expression was determined by immunoblotting with specific antibodies. As shown in Figure 1, clear induction of the genes encoding ALK3^{CA}, ALK5^{CA} and ALK6^{CA} was observed by immunoblotting with anti-HA (Figure 1A), and Smad1 and 6, by anti-Flag (Figure 1B). ALK3^{CA} or ALK6^{CA} overexpression induced phosphorylation of Smad1, Smad5, and Smad8 in SFs, and ALK5^{CA}-transduced cells showed Smad2 phosphorylation (Figure 1A). MKK6^{CA} virus infection specifically activated p38 pathways in SFs, and the pathways were also activated in ALK3^{CA}-transduced cells as determined by Western blotting with anti-phospho-p38 (Figure 1C). The increased p38 phosphorylation induced by either ALK3^{CA} or MKK6^{CA} overexpression was suppressed by the p38-selective inhibitor SB203580.

Induction of chondrocyte-specific gene expression by ALK3^{CA} transduction in pellet cultures of SFs. To determine the effects of these transduced gene products on chondrocyte-specific gene expression in SFs, we subjected infected cells to pellet culture. After 7 days of culture, clear induction of type II collagen and aggrecan genes was observed in ALK3^{CA}-transduced cultures by both Northern blot analysis (Figure 2A) and real-time PCR (Figure 2, B and C). Expression of these genes was also observed in ALK6^{CA}-transduced cultures, albeit less efficiently, as shown in Figure 2, B and C, by real-time PCR. Contrary to the strong chondrogenic effects of ALK3^{CA} virus, expression
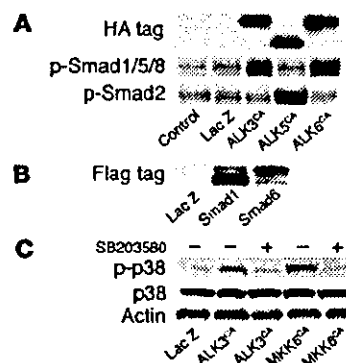
Figure 1
Modulation of intracellular signaling pathways by adenovirus vector–mediated gene transduction into SFs. (A) SFs at passage 3 were transduced with HA-tagged constitutively active ALK3, ALK5, and ALK6, and the expressed products were detected by immunoblotting after 2 days of viral infection. Expression of these genes was detected by immunoblotting with anti-HA and phospho-Smad1, -Smad 5, and Smad8 (p-Smad1/5/8) was observed in cells expressing ALK3^{CA} or ALK6^{CA}, and p-Smad2, in cells expressing ALK5^{CA}. (B) Expression of Smad1 and 6 in SFs was determined by anti-Flag. (C) Adenovirus vector–mediated ALK^{CA} or MKK6^{CA} expression specifically activated p38 pathways in SFs, as determined by Western blotting with anti-phospho-p38 (p-p38). The increased p38 phosphorylation induced by ALK3^{CA} or MKK6^{CA} overexpression was suppressed by the p38-selective inhibitor SB203580.
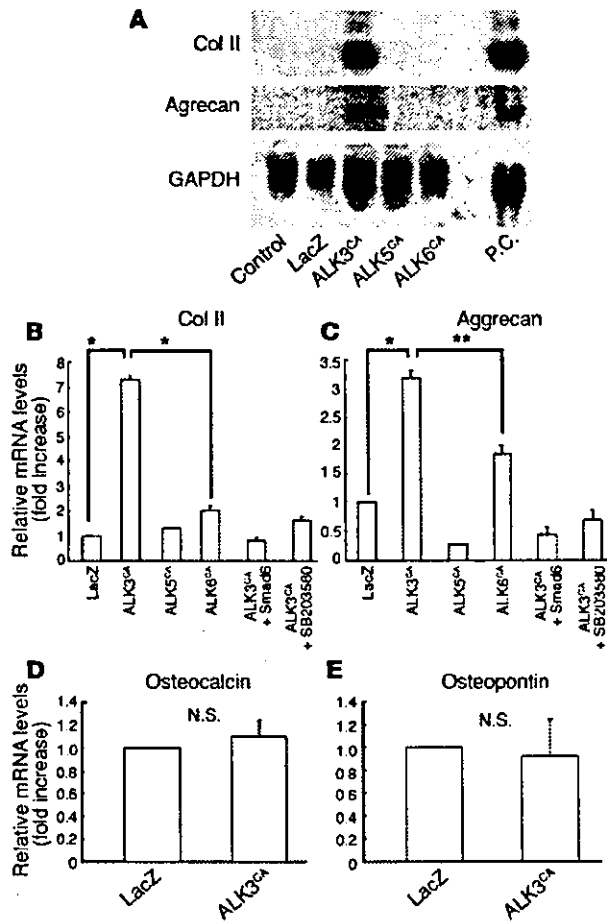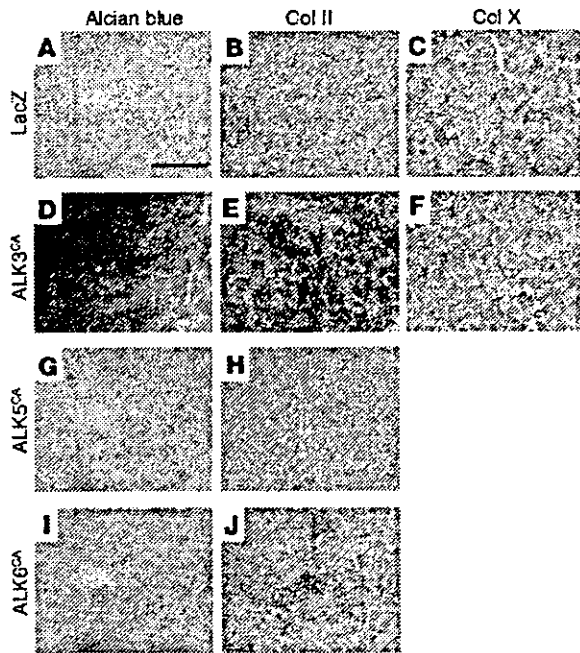
Figure 2
Effects of ALK3^{CA}, ALK5^{CA}, and ALK6^{CA} expression on chondrocyte-specific gene expression in SFs. (A–E) Gene expression in SFs, as determined by Northern blot analysis (A) and real-time PCR analysis (B–E). Subconfluent monolayer SF cultures were infected with adenovirus vectors and they were then subjected to pellet culture 24 hours after viral infection; mRNA extracted from the pellets after 7 days of culture was then analyzed. Expression of type II collagen (Col II) and aggrecan was clearly induced in ALK3^{CA}-expressing cultures, as shown by Northern blot analysis (A) and real-time PCR analysis (B and C); this was suppressed by Smad6 coexpression and SB203580 (B and C). Expression of type II collagen and aggrecan was also observed in ALK6^{CA}-expressing cultures, albeit less efficiently, as shown in B and C by real-time PCR. Neither the osteocalcin nor the osteopontin gene was induced by ALK3^{CA} virus infection (D and E). P.C., positive control, which represents the Northern blotting using mRNA of primary chondrocytes. N.S., not significant; *P < 0.001; **P < 0.005 (significantly different).

of osteocalcin or osteopontin was hardly detectable in the cells (Figure 2, C and D), indicating that hypertrophic and osteogenic differentiation were somehow blocked in these cultures. In contrast, neither type II collagen nor aggrecan gene expression was observed in ALK5^{CA} virus-infected cells (Figure 2, A–C). Type II collagen and aggrecan expression induced by ALK3^{CA} transduction was completely suppressed by coexpression with Smad6 or by SB203580 (Figure 2, B and C).

ALK3 gene transduction increases Alcian blue–positive matrix and type II collagen deposition in pellet cultures of SFs. For histological analysis, cells were subjected to pellet culture 24 hours after the viral infection. After 3 weeks of pellet culture, cells were fixed and examined by Alcian blue staining (Figure 3, A, D, G, and I) and Alizarin red staining and type II collagen immunostaining (Figure 3, B, E, G, and J) and type X collagen immunostaining (Figure 3, C and F). ALK3^{CA} virus-infected cultures showed cartilageous matrix production that was strongly positive for Alcian blue staining (Figure 3D), while no positive staining was observed in LacZ virus-infected cultures (Figure 3A) or ALK5^{CA} virus-infected cultures (Figure 3G), and only weak staining was observed in ALK6^{CA} virus-infected cultures (Figure 3H). No Alizarin red staining was observed in ALK3^{CA}-infected cultures (not shown), indicating that mineralization associated with osteogenic differentiation was not induced. ALK3^{CA} virus-infected SFs showed an oval shape, morphologically reminiscent of chondrocytes (Figure 3D). Immunostaining with

anti–type II collagen showed positive staining in ALK3^{CA} virus-infected pellet cultures (Figure 3E) and weak staining in ALK6^{CA} virus-infected cultures (Figure 3H), while we failed to detect type X collagen in ALK3^{CA} virus-infected cultures (Figure 3F), which suggests an absence of terminal differentiation to hypertrophic chondrocytes. No positive type II collagen immunostaining was detected in LacZ virus-infected cultures (Figure 3B) or ALK5^{CA} virus-infected cultures (Figure 3H).

ALK3^{CA}-transduced SFs after pellet culture form cartilage matrix in vivo. To study chondrogenic differentiation of SFs in vivo, we subcutaneously transplanted the pellets into nude mice. Mice were sacrificed 3 weeks after the transplantation and the pellets were recovered and subjected to histological analysis. The transplanted SF pellets expressing ALK3^{CA} were positively stained for toluidine blue (Figure 4C), which detects proteoglycan components, as does Alcian blue staining. Type II collagen immunostaining was also positive (Figure 4D), indicating the cartilaginous differentiation of the cultures in vivo, while Alizarin red staining was almost undetectable (data not shown). ALK6^{CA} expression also induced chondrogenesis, albeit much less prominently (not shown), while neither LacZ (Figure 4, A and B) or ALK5^{CA} (not shown) expression could induce chondrogenic phenotypes in the cultures. The histological observation was further confirmed by real-time PCR; expression of type II collagen and aggrecan was significantly higher in ALK3^{CA}-transduced pellets (Figure 4, E and F). These results suggest that ALK3^{CA}

−423−

Figure 3
ALK3^CA gene transduction increases Alcian blue–positive matrix and type II collagen deposition in pellet cultures of SFs. (A–J) Adenovirus-infected SF pellets were fixed with 3.7% formaldehyde after 3 weeks of culture and then were subjected to Alcian blue staining (A, D, G, and I) or immunostaining with anti–type II collagen (B, E, H, and J) or anti–type X collagen (Col X) (C and F). Distinct Alcian blue (D) and type II collagen (E) staining was observed in ALK3^CA-expressing cultures. ALK6^CA-expressing cultures showed weaker staining (I and J), and no positive staining was observed in ALK5^CA virus–infected (G and H) or LacZ virus–infected (A and B) cultures. No type X collagen immunostaining was observed in cultures expressing LacZ or ALK3^CA (C and F). Scale bar: 100 μm.

overexpression was able to target cartilage formation without subsequent bone formation in vivo.
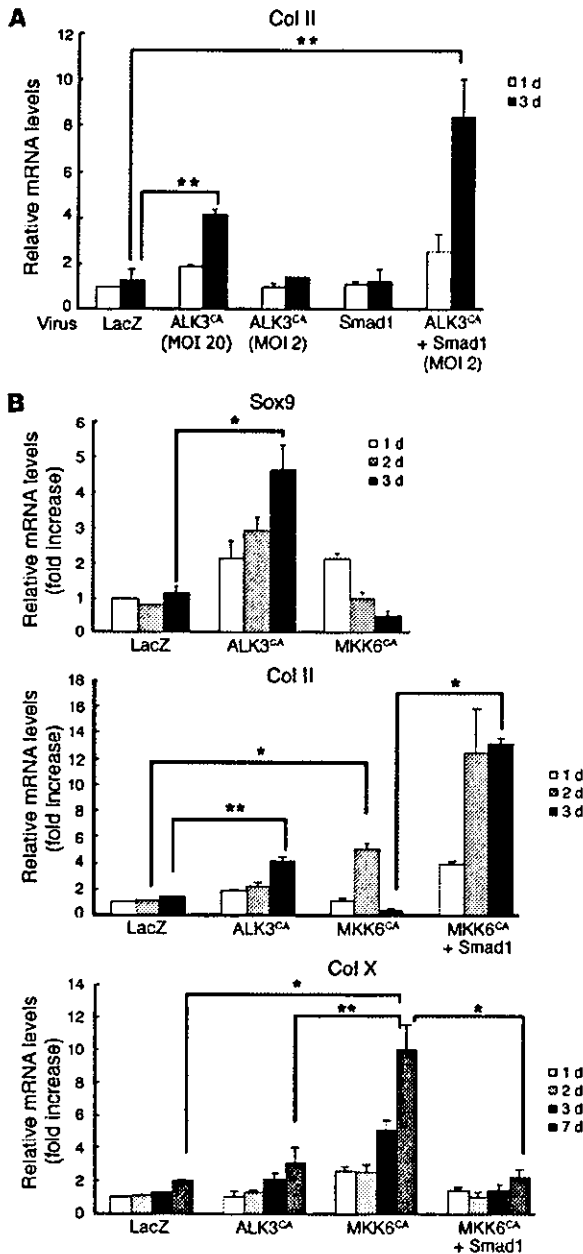
Segregation of ALK signaling pathways. ALK signaling is known to be mediated by both the Smad pathways and MAP kinase pathways, especially the p38 pathways (31–33). We therefore attempted to distinguish the roles of the Smad pathways and p38 pathways from each other using a specific p38 inhibitor or adenovirus vectors. Smad6 coexpression or treatment of the cultures with the p38 inhibitor SB203580 completely abrogated the chondrogenic gene expression induced by ALK3^CA (Figure 2, B and C). These results indicate that both the Smad pathways and the p38 MAP kinase pathways are required for the differentiation. Although Smad1 expression alone (MOI = 20) or a small amount of ALK^CA virus (MOI = 2) failed to induce type II collagen expression in SFs, both had synergistic effects, and robust upregulation of type II collagen gene was observed by coinfection of Smad1 virus (MOI = 20) and ALK3^CA virus (MOI = 2) (Figure 5A). Interestingly, activation of p38 pathways alone by MKK6^CA expression in SFs induced rapid induc-

tion of Sox9 and type II collagen, which declined rapidly, however, and type X collagen expression was subsequently increased (Figure 5B). Coexpression of Smad1 together with MKK6^CA not only reduced type X collagen expression but also maintained type II collagen expression in the cells (Figure 5B). Pellet cultures infected

Figure 4
ALK3^CA-transduced SFs form cartilage matrix in vivo. (A–D) Three weeks after transplantation into nude mice, pellets were recovered and stained with toluidine blue (A and C) and immunostained with anti–type II collagen (B and D). Type II collagen immunohistochemistry was shown in the enlarged features of the rectangular area in the toluidine blue staining. Distinct positive staining was observed in ALK3^CA-expressing cultures (B and D) in contrast to LacZ virus–infected cultures (A and C). Scale bars: 100 μm. (E and F) Real-time PCR analysis of type II collagen and aggrecan. Their expression was significantly higher in ALK3^CA-expressing pellets than in LacZ-expressing pellets. *P < 0.001 (significantly different).

A

Col II

B

Sox9

Col II

Col X
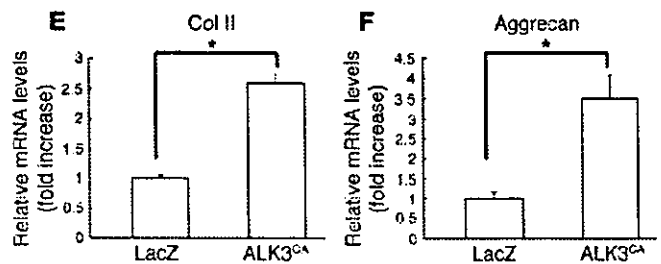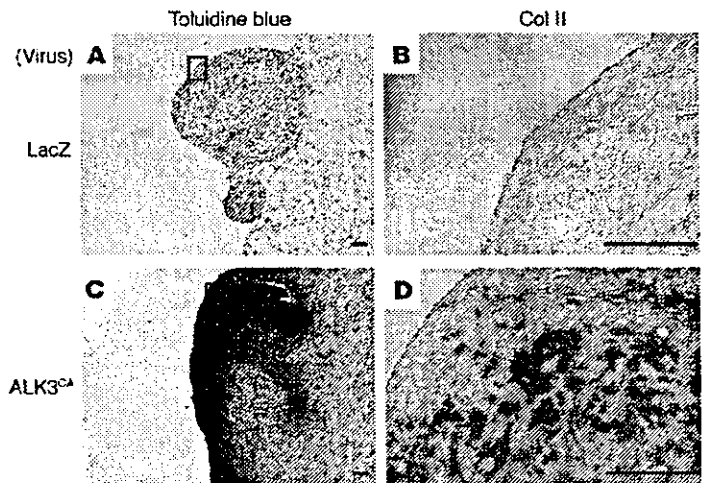
Figure 5
Segregation of downstream signaling pathways of ALK3. (A) Synergistic effect of Smad1 expression on the chondrogenic effects of the ALK3^{CA} virus. Expression of Smad1 (MOI = 20) together with ALK3^{CA} virus (MOI = 2) strongly induced expression of type II collagen in SFs. White bars indicate type II collagen expression on day 1 of cultures, and black bars indicate that on day 3. **P < 0.005 (significantly different). (B) MKK6-p38 pathways promote terminal chondrocytic differentiation of SFs. Mandatory activation of p38 pathways by expression of MKK6^{CA} using adenovirus vectors rapidly activated expression of the Sox9 and type II collagen genes, which rapidly declined, while expression of a terminal chondrocytic differentiation marker, type X collagen, was gradually increased. Adenovirus vector–mediated overexpression of Smad1 together with MKK6^{CA} suppressed type X collagen expression and maintained type II collagen expression in SFs. *P < 0.001; **P < 0.005 (significantly different).

Clusters of migrating synovial cells were observed adjacent to the osteochondrophytes (Figure 7B, arrowheads), where future osteochondrophytes will develop, and they were weakly stained by toluidine blue and anti-type X collagen at the marginal area between synovium and osteophytes (rectangular areas in Figure 7, B and D). This region was also positively stained by anti-phospho-p38 (Figure 7F). No positive staining was observed in the normal synovium, however (data not shown).

Discussion
The signaling events leading to chondrogenesis still remain elusive, although there is accumulating evidence that TGF-β superfamily cytokines may play an important role (19–22). The receptors of TGF-β family members are composed of two different types of serine/threonine kinase receptors, known as type I and type II (31, 34, 35). Type II receptors are constitutively active kinases and phosphorylate type I receptors, also called ALKs. Type I receptors in turn mediate specific intracellular signaling pathways and therefore determine the specificity of the downstream signaling. So far, seven type I receptors have been identified, ALKs 1-7. ALK3 (BMPR-IA) and ALK6 (BMPR-IB) are structurally similar to each other and function as BMP receptors, while ALK5 and ALK4 work as type I TGF-β receptors. Using the adenovirus vector system, Fujii et al. reported that ALK1^{CA}, ALK2^{CA}, ALK3^{CA}, and ALK6^{CA} induced osteoblastic differentiation of C2C12 myoblasts and that ALK3^{CA} or ALK6^{CA} introduction induced chondrocytic differentiation of ATDC teratocarcinoma cells (27).

In the present study, we focused on the regulation of chondrogenic differentiation of primary SFs obtained from rheumatoid arthritis patients. SFs have chondrogenic potential (15, 16) and can migrate into articular cartilage defects, where they deposit a scar-like tissue as Hunziker et al. pointed out (14), suggesting that SFs have anabolic effects on joint homeostasis and are involved in the restoration process of articular cartilage. We demonstrated that adenovirus vector–mediated ALK3^{CA} gene expression induced robust induction of chondrocyte-specific gene expression in SFs in a ligand-independent manner. Clear induction of Sox9, a key transcription factor regulating chondrogenesis (36, 37), followed by type II collagen and aggrecan expression, was observed in the ALK3^{CA}-expressing cultures, while type X collagen was only weakly induced in the cultures and no osteocalcin expression could be found (Figures 2 and 5). Induction of these chondrocyte-specific genes through ALK3^{CA} expression was not observed in skin fibroblasts, suggesting the cell specificity of the events (data not

with MKK6^{CA} virus were positively stained by type X collagen immunostaining as well as Alizarin red staining, which was suppressed by Smad1 virus coinfection (Figure 6).

Type X collagen expression and p38 activation in synovial cells in osteoarthritic joints. To examine the role of p38 activation in the development of degenerative changes in the articular cartilage, we next analyzed synovial tissues in the mouse model of osteoarthritis. After ACL and MM resection, the animals developed degenerative joint changes mimicking osteoarthritis. Osteochondrophytes were formed at the posterior edge of the femoral condyle and they were positively stained by anti-type X collagen as well as toluidine blue (rectangular areas in Figure 7, A and C) 4 weeks after the operation (corresponding to the stage of moderate osteoarthritis).
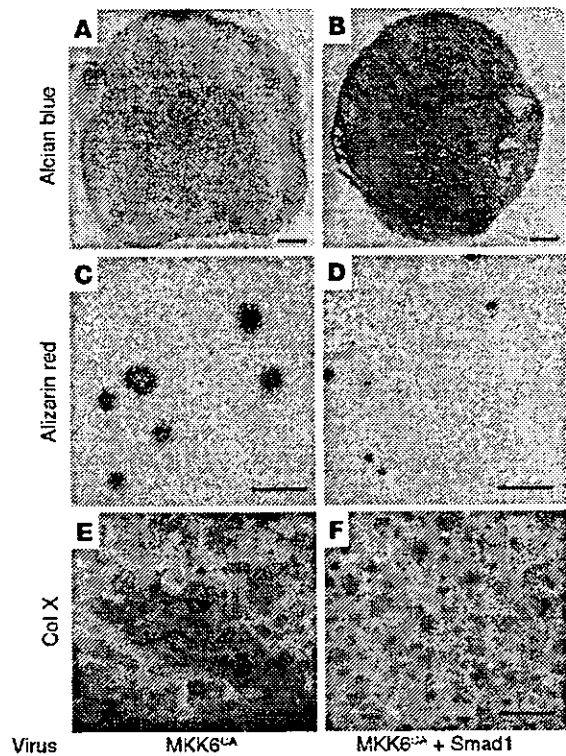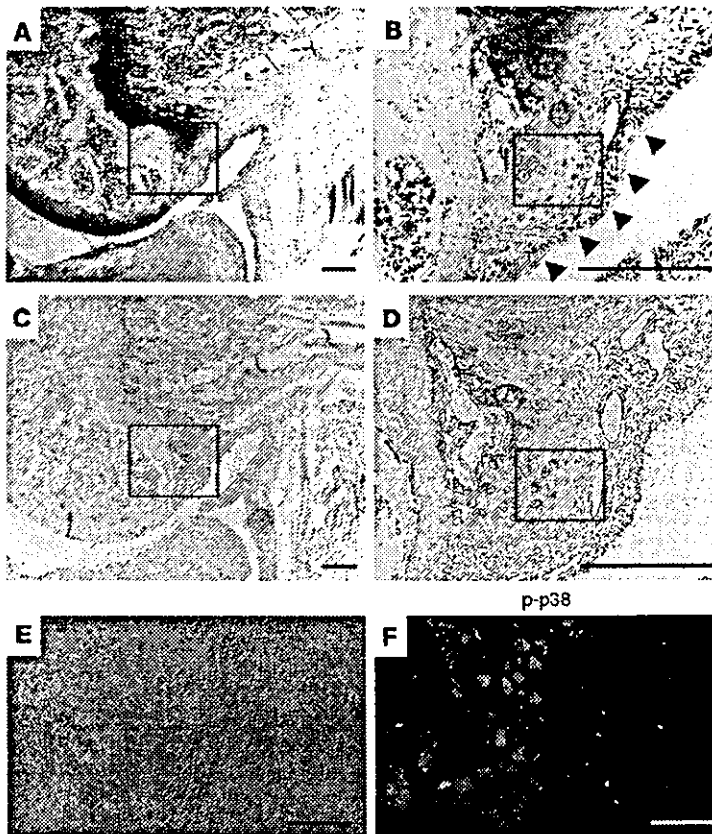
Figure 6
Induction of Alizarin red staining and type X collagen in MKK6-transduced SFs in pellet cultures. (A–F) SFs infected with MKK6CA virus alone (A, C, and E) or together with Smad1 virus (B, D, and F) were subjected to pellet culture. Cultures were fixed with 3.7% formaldehyde 3 weeks later, and then stained with Alcian blue (A and B), Alizarin red (C and D) or anti–type X collagen (E and F). Note the increased Alcian blue staining and the reduced Alizarin red activity and type X collagen immunoactivity with Smad1 coexpression. Scale bars:100 μm (A–D) and 50 μm (E and F).

shown). The chondrogenic effect of ALK3CA virus was further confirmed histologically by pellet cultures performed in vitro and in vivo (Figures 3 and 4). Induction of neither the osteoblast markers osteopontin and osteocalcin nor the terminal chondrocyte differentiation markers type X collagen and mineralization was observed in ALK3CA-expressing cells (Figures 2, 3, 5, and 6). These results suggest that ALK3 signaling, that is, BMP signaling, has both stimulatory and regulatory roles in chondrogenesis: to induce the chondrogenic differentiation of SFs and at the same time to block their osteoblastic or hypertrophic differentiation. Despite the structural similarity between ALK3 and ALK6, the ALK6CA virus was much less efficient in chondrogenesis, the reason for which remains to be clarified. Although many studies have demonstrated a prochondrogenic effect for TGF-β (15, 16, 20–22), we failed to find an anabolic effect for ALK5CA which is expected to mimic TGF-β signaling, on the chondrogenic differentiation of SFs. We cannot fully explain the discrepancy between our results and those of previous studies, but Robbins and coworkers recently reported that adenovirus vector–mediated TGF-β gene transduction into arthritic joints in fact exacerbated cartilage degradation (38), raising the possibility that sustained activation of TGF-β signaling, via ALK5, has instead a negative effect on chondrogenesis. Further study will be required to elucidate the difference between TGF-β and BMP signaling.

The signaling of TGF-β/BMPs is transduced by Smad family members (31, 34, 35). Receptor-regulated Smads (R-Smads) are direct substrates of type I receptors and are phosphorylated at the C-terminal SSV/MS motif. R-Smads then form heteromeric complexes with common-mediator Smads and translocate into the nuclei, where they regulate transcription of target genes. In addition to Smad pathways, there is evidence that MAP kinase

cascades are also implicated in ALK signaling, in which TGF-β–activating kinase (TAK1), a member of the MAP kinase kinase kinase family, plays a key role. TAK1 activates MAP kinase kinase in combination with an adaptor molecule, TAB1, which leads to JNK and p38 activation (32). The role of p38 in chondrogenesis has recently attracted particular interest because p38 inhibitors such as SB203580 suppress the chondrogenic differentiation of ATDC5 cells induced by growth/differentiation factor-5 (33, 39). However, the exact roles of the Smad pathways and p38 pathways in chondrocyte differentiation are not yet fully clarified. We used a combination of adenoviral gene delivery and a chemical inhibitor to segregate the roles of these two pathways downstream of ALK3 activation and found that (a) inhibitory Smad (Smad6) expression or treatment with the p38 inhibitor SB203580 suppressed the effect of ALK3CA expression (Figure 2) (b) Smad1 synergistically augmented the effect of ALK3CA (Figure 5A), and (c) activation of p38 pathways alone by MKK6CA expression induced the hypertrophic differentiation markers type X collagen and mineralization in SFs, which was suppressed by Smad1 coexpression (Figures 5B and 6). These results suggest that although both Smad and p38 activation is necessary for chondrogenic differentiation of SFs, sustained activation of p38 pathways alone prompts the terminal differentiation of the cells. Consistent with our results, Zhen et al. (40) reported that parathyroid hormone inhibits type X collagen expression in hypertrophic chondrocytes by suppressing p38 pathways. Von der Mark et al. (41) reported the focal appearance of type X collagen in osteoarthritic cartilage, which may be involved in the degenerative changes of the articular cartilage and in the pathogenesis of osteoarthritis. Using the mouse model of osteoarthritis, we found that activated p38 is associated with type X colla-

—426—

Figure 7
Histological analysis of knee joints in the mouse ACL and MM resection model. (A–F) Toluidine blue staining (A and B) and type X collagen immunostaining (C and D) at the marginal area between the articular cartilage and synovium. B and D present higher-magnification views of A and C, respectively. Osteochondrophytes were formed at the posterior edge of the femoral condyle, and they were positively stained by anti–type X collagen as well as toluidine blue (rectangular areas in A and C). Clusters of migrating synovial cells were observed adjacent to the osteochondrophytes (B, arrowheads) where future osteochondrophytes will develop, and they were positively stained by anti–type X collagen at the marginal area between synovium and osteophytes (rectangular area in D). This region was also positively stained by anti–phospho-p38 (F). E and F represent phase-contrast microscopy (E) and immunostaining with anti–phospho-p38 (F) of the rectangular area in D. Positive phospho-p38 staining was observed at the area of osteochondrophytes as well as the marginal synovium. Scale bars: 500 μm (A–D) and 50 μm (E and F).

gen expression in the synovial tissues adjacent to osteochondrophytes as well as in the degenerative cartilage (Figure 7).

Smad pathways not only are required for chondrogenic differentiation of SFs but also critically regulate the stage of differentiation of the cells and suppress their terminal differentiation process. Consistent with our findings, Scharstuhl recently reported inhibitory action of Smad7 in TGF-β–induced chondrocyte proliferation and proteoglycan production (42), indicating a critical role for Smad pathways. Hidaka and coworkers (43) demonstrated that adenovirus vector–mediated BMP-7 expression in chondrocytes accelerates the cartilage repair process. More recently, Lories and colleagues (44) demonstrated that BMP-2 and BMP-6 expressed in arthritic synovium are regulated by proinflammatory cytokines and differentially modulate fibroblast-like synoviocyte apoptosis, and Fukui et al. (45) found that BMP-2 expression was increased by proinflammatory cytokines in normal and osteoarthritis chondrocytes. These findings, combined with our observations, suggest that although BMPs have favorable effects on the repair process of articular cartilage, they may have proapoptotic and/or degenerative effects on the cells when p38 pathways are overactivated. Our findings suggest an important role for p38 signal transduction pathways in chondrocytes and SFs, leading to degenerative joint disorders, and suggest the potential utility of p38 modifiers in the treatment of rheumatoid arthritis and/or osteoarthritis. In fact, p38 kinase modifiers are now in clinical trials to treat rheumatoid arthritis (46). Based on our observations, we would like to propose that SFs are an excellent source for chondroprogenitors, which can

be differentiated into chondrocytes via ALK3 activation, and that activation of the Smad pathway while controlling the degree of p38 activation may be a way to generate committed chondrocytes for the repair and/or replacement of cartilage.

Address correspondence to: Sakae Tanaka, Department of Orthopaedic Surgery, Faculty of Medicine, The University of Tokyo, 7-3-1 Hongo, Bunkyo-ku, Tokyo 113-0033, Japan. Phone: 81-3-3815-5411 ext. 33376; Fax: 81-3-3818-4082; E-mail: TANAKAS-ORT@h.u-tokyo.ac.jp.

1. Hunziker, E.B. 2002. Articular cartilage repair: basic science and clinical progress. A review of the current status and prospects. *Osteoarthritis Cartilage* 10:432-463.

2. Poole, A.R., et al. 2001. Composition and structure of articular cartilage: a template for tissue repair. *Clin. Orthop.* 391:S26-S33.

3. Poole, A.R. 2003. What type of cartilage repair are we attempting to attain? *J. Bone Joint Surg. Am.* 85-A(Suppl. 2):40-44.

4. Hunziker, E.B. 2003. Tissue engineering of bone and cartilage. From the preclinical model to the patient. *Novartis Found. Symp.* 249:70-85, 170-174, and 239-141.

5. Bruder, S.P., et al. 1998. Mesenchymal stem cells in osteobiology and applied bone regeneration. *Clin. Orthop.* 355:S247-S256.

6. Matsusue, Y., Yamamuro, T., and Hama, H. 1993. Arthroscopic multiple osteochondral transplantation to the chondral defect in the knee associated with anterior cruciate ligament disruption. *Arthroscopy.* 9:318-321.

7. Bentley, G., et al. 2003. A prospective, randomised comparison of autologous chondrocyte implantation versus mosaicplasty for osteochondral defects in the knee. *J. Bone Joint Surg. Br.* 85:223-230.

8. Peterson, L., Minas, T., Brittberg, M., and Lindahl, A. 2003. Treatment of osteochondritis dissecans of the knee with autologous chondrocyte transplantation: results at two to ten years. *J. Bone Joint Surg Am.* 85-A(Suppl 2):17-24.

9. Peterson, L., Brittberg, M., Kiviranta, I., Akerlund, E.L., and Lindahl, A. 2002. Autologous chondrocyte transplantation. Biomechanics and long-term durability. *Am. J. Sports Med.* 30:2-12.

10. Minas, T., and Nehrer, S. 1997. Current concepts in the treatment of articular cartilage defects. *Orthopedics.* 20:525-538.

11. Hangody, L., Feczko, P., Bartha, L., Bodo, G., and Kish, G. 2001. Mosaicplasty for the treatment of articular defects of the knee and ankle. *Clin. Orthop.* 391:S328-S336.

12. Firestein, G.S. 2003. Evolving concepts of rheumatoid arthritis. *Nature.* 423:356-361.

13. Takayanagi, H., et al. 1999. Suppression of arthritic bone destruction by adenovirus-mediated csk gene transfer to synoviocytes and osteoclasts. *J. Clin. Invest.* 104:137-146.

14. Hunziker, E.B., and Rosenberg, L.C. 1996. Repair of partial-thickness defects in articular cartilage: cell recruitment from the synovial membrane. *J. Bone Joint Surg. Am.* 78:721-733.

15. Nishimura, K., et al. 1999. Chondroprogenitor cells of synovial tissue. *Arthritis Rheum.* 42:2631-2637.

16. De Bari, C., Dell'Accio, F., Tylzanowski, P., and Luyten, F.P. 2001. Multipotent mesenchymal stem cells from adult human synovial membrane. *Arthritis Rheum.* 44:1928-1942.

17. De Bari, C., et al. 2003. Skeletal muscle repair by adult human mesenchymal stem cells from synovial membrane. *J. Cell Biol.* 160:909-918.

18. O'Connell, J.X. 2000. Pathology of the synovium. *Am. J. Clin. Pathol.* 114:773-784.

19. Wozney, J.M. 1989. Bone morphogenetic proteins. *Prog. Growth Factor Res.* 1:257-280.

20. Kulyk, W.M., Rodgers, B.J., Greer, K., and Kosher, R.A. 1989. Promotion of embryonic chick limb cartilage differentiation by transforming growth factor-beta. *Dev. Biol.* 135:424-430.

21. Lafeber, F.P., Vander Kraan, P.M., Van Roy, J.L., Huber-Bruning, O., and Bijlsma, J.W. 1993. Articular cartilage explant culture; an appropriate in vitro system to compare osteoarthritic and normal human cartilage. *Connect. Tissue Res.* 29:287-299.

22. Denker, A.E., Nicoll, S.B., and Tuan, R.S. 1995. Formation of cartilage-like spheroids by micromass cultures of murine C3H10T1/2 cells upon treatment with transforming growth factor-beta 1. *Differentiation.* 59:25-34.

23. Yamamoto, A., et al. 2003. Suppression of arthritic bone destruction by adenovirus-mediated dominant-negative Ras gene transfer to synoviocytes and osteoclasts. *Arthritis Rheum.* 48:2682-2692.

24. Takayanagi, H., et al. 2000. Involvement of receptor activator of nuclear factor kB ligand/osteoclast differentiation factor in osteoclastogenesis from synoviocytes in rheumatoid arthritis. *Arthritis Rheum.* 43:259-269.

25. Tanaka, S., et al. 1998. Modulation of osteoclast function by adenovirus vector-induced epidermal growth factor receptor. *J. Bone Miner. Res.* 13:1714-1720.

26. Miyake, S., et al. 1996. Efficient generation of recombinant adenoviruses using adenovirus DNA-terminal protein complex and a cosmid bearing the full-length virus genome. *Proc. Natl. Acad. Sci. U. S. A.* 93:1320-1324.

27. Fujii, M., et al. 1999. Roles of bone morphogenetic protein type I receptors and Smad proteins in osteoblast and chondroblast differentiation. *Mol. Biol. Cell.* 10:3801-3813.

28. Enomoto-Iwamoto, M., et al. 2000. Hedgehog proteins stimulate chondrogenic cell differentiation and cartilage formation. *J. Bone Miner. Res.* 15:1659-1668.

29. Kamekura, S., et al. 2003. Establishment of novel experimental osteoarthritis models in mice. *J. Bone Miner. Res.* 18:S395.

30. van den Berg, W.B. 2001. Lessons from animal models of osteoarthritis. *Curr. Opin. Rheumatol.* 13:452-456.

31. Derynck, R., Zhang, Y., and Feng, X.H. 1998. Smads: transcriptional activators of TGF-beta responses. *Cell.* 95:737-740.

32. Miyazono, K., Kusanagi, K., and Inoue, H. 2001. Divergence and convergence of TGF-beta/BMP signaling. *J. Cell Physiol.* 187:265-276.

33. Watanabe, H., de Caestecker, M.P., and Yamada, Y. 2001. Transcriptional cross-talk between Smad, ERK1/2, and p38 mitogen-activated protein kinase pathways regulates transforming growth factor-beta-induced aggrecan gene expression in chondrogenic ATDC5 cells. *J. Biol. Chem.* 276:14466-14473.

34. Miyazono, K. 1997. TGF-beta receptors and signal transduction. *Int. J. Hematol.* 65:97-104.

35. Massague, J. 1998. TGF-beta signal transduction. *Annu. Rev. Biochem.* 67:753-791.

36. de Crombrugghe, B., et al. 2000. Transcriptional mechanisms of chondrocyte differentiation. *Matrix Biol.* 19:389-394.

37. Akiyama, H., Chaboissier, M.C., Martin, J.F., Schedl, A., and de Crombrugghe, B. 2002. The transcription factor Sox9 has essential roles in successive steps of the chondrocyte differentiation pathway and is required for expression of Sox5 and Sox6. *Genes Dev.* 16:2813-2828.

38. Mi, Z., et al. 2003. Adverse effects of adenovirus-mediated gene transfer of human transforming growth factor beta 1 into rabbit knees. *Arthritis Res.* 5:R132-R139.

39. Nakamura, K., et al. 1999. p38 mitogen-activated protein kinase functionally contributes to chondrogenesis induced by growth/differentiation factor-5 in ATDC5 cells. *Exp. Cell Res.* 250:351-363.

40. Zhen, X., Wei, L., Wu, Q., Zhang, Y., and Chen, Q. 2001. Mitogen-activated protein kinase p38 mediates regulation of chondrocyte differentiation by parathyroid hormone. *J. Biol. Chem.* 276:4879-4885.

41. von der Mark, K., et al. 1995. Upregulation of type X collagen expression in osteoarthritic cartilage. *Acta Orthop. Scand. Suppl.* 266:125-129.

42. Scharstuhl, A., et al. 2003. Adenoviral overexpression of Smad-7 and Smad-6 differentially regulates TGF-beta-mediated chondrocyte proliferation and proteoglycan synthesis. *Osteoarthritis Cartilage.* 11:773-782.

43. Hidaka, C., et al. 2003. Acceleration of cartilage repair by genetically modified chondrocytes over expressing bone morphogenetic protein-7. *J. Orthop. Res.* 21:573-583.

44. Lories, R.J., Derese, I., Ceuppens, J.L., and Luyten, F.P. 2003. Bone morphogenetic proteins 2 and 6, expressed in arthritic synovium, are regulated by proinflammatory cytokines and differentially modulate fibroblast-like synoviocyte apoptosis. *Arthritis Rheum.* 48:2807-2818.

45. Fukui, N., Zhu, Y., Maloney, W.J., Clohisy, J., and Sandell, L.J. 2003. Stimulation of BMP-2 expression by pro-inflammatory cytokines IL-1 and TNF-alpha in normal and osteoarthritic chondrocytes. *J. Bone Joint Surg. Am.* 85-A(Suppl. 3):59-66.

46. Pargellis, C., and Regan, J. 2003. Inhibitors of p38 mitogen-activated protein kinase for the treatment of rheumatoid arthritis. *Curr. Opin. Investig. Drugs.* 4:566-571.

Differential regulation of Th1 responses and CD154 expression in human CD4+ T cells by IFN-α

H. SHIBUYA*†, T. NAGAI*†, A. ISHII†, K. YAMAMOTO‡ & S. HIROHATA* *Department of Internal Medicine, Teikyo University School of Medicine, Tokyo, and †Department of Respiratory Medicine and ‡Department of Allergy and Rheumatology, University of Tokyo Graduate School of Medicine, Tokyo, Japan

SUMMARY

Like interleukin (IL)-12, interferon (IFN)-α has been shown to play an important role in inducing human Th1 responses. Recent studies have shown that human Th1 responses driven by IL-12 are associated with enhanced expression of CD154. The present study examined the effects of IFN-α on CD154 expression in human CD4+ T cells, with special attention to the relationship with Th1 responses. Highly purified CD4+ T cells from healthy donors were stimulated with immobilized anti-CD3 with or without IFN-α and IL-12 in the complete absence of accessory cells. IFN-α suppressed CD154 protein and mRNA expression in CD4+ T cells at the initial phase of activation with immobilized anti-CD3, but enhanced it in the subsequent maturation phase irrespective of the presence of IL-12. By contrast, IFN-α by itself did not enhance IFN-γ production or mRNA expression in CD4+ T cells in the absence of IL-12 even in the presence of stimulation with anti-CD28, but enhanced it in the presence of IL-12. Accordingly, IFN-α enhanced IL-12Rβ2 mRNA expression in anti-CD3-stimulated CD4+ T cells. Neither IFN-α nor IL-12 influenced the stability of CD154 mRNA in anti-CD3-activated CD4+ T cells. These results indicate that IFN-α by itself enhances CD154 expression in CD4+ T cells independently of the induction of IFN-γ mRNA expression. The data also suggest that the optimal induction of human Th1 responses by IFN-α might require the presence of IL-12 and that the induction of Th1 responses and CD154 expression in human CD4+ T cells might be regulated through different mechanisms.

Keywords anti-CD3 cytokines cell surface molecules Th1/ Th2

INTRODUCTION

Interleukin (IL)-12 is a heterodimeric cytokine composed of 40-kDa (p40) and 35-kDa (p35) subunits, produced by macrophages, B cells, and dendritic cells (DCs) [1,2]. One of the most important roles of IL-12 in immune regulation is to induce the differentiation of Th1 cells from naive CD4+ T cells [3,4]. Previous studies showed that IL-12 up-regulates CD154 expression on human T cells at the protein level [5,6] as well as at the mRNA level [5]. It was therefore suggested that human Th1 responses driven by IL-12 might be associated with enhanced expression of CD154 [6]. However, it remains unclear whether the enhanced CD154 expression might be the sequelae of Th1 responses or a chanced association, as the precise mechanism of the enhancement of CD154 expression on human T cells by IL-12 has not been elucidated.

Correspondence: Dr Shunsei Hirohata, Department of Internal Medicine, Teikyo University School of Medicine, 2-11-1 Kaga, Itabashi-ku, Tokyo 173-8605, Japan.
E-mail: shunsei@med.teikyo-u.ac.jp

Interferon (IFN)-α is a member of a multigene family, which presents potent antiviral actions as well as immunoregulatory activities, such as the enhancement of cytotoxic activity of T cells and natural killer (NK) cells [7]. IFN-α is produced by macrophages, DCs and fibroblasts and its production is enhanced prominently during viral and bacterial infection [7]. The immune modulating functions of IFN-α suggest that IFN-α may be an important link between innate and adaptive immune responses [8]. Like IL-12, IFN-α has also been shown to activate Stat4 [9,10] and induce Th1 development directly in humans [10]. Because IL-12 induces Th1 responses as well as the enhancement of CD154 expression, it is possible that IFN-α might also influence CD154 expression in human T cells. In fact, several studies have demonstrated that IFN-α results in the development of lupus-like autoimmunity [11–13], in which abnormal expression of CD154 might be involved [14,15]. Thus, it is highly likely that IFN-α might enhance CD154 expression. However, the effects of IFN-α on CD154 expression in human T cells have not been elucidated.

216

The current studies were therefore undertaken to explore the effects of IFN-α on CD154 expression in activated human CD4⁺ T cells, utilizing a system with immobilized anti-CD3, which permits stimulation of all peripheral blood T cells in the complete absence of accessory cells. This system therefore enables us to evaluate the effects of IFN-α on CD4⁺ T cells without any effects of endogenous IL-12 produced by accessory cells or B cells. Special attention was directed to the relationship between CD154 expression and induction of Th1 responses.

MATERIALS AND METHODS

Monoclonal antibodies (MoAbs) and reagents
A variety of MoAbs were used, including 64·1 (a gift of Dr P. E. Lipsky, National Institute of Health, Bethesda, MD, USA), an IgG2a MoAb directed at the CD3 molecule on mature T cells; fluorescein isothiocyanate (FITC)-conjugated anti-CD154 (a murine IgG1 MoAb, clone 24–31) (Ancell, Bayport, MN, USA); phycoerythrin (PE)-conjugated anti-IL-2 receptor α-chain (CD25) (a murine IgG2a MoAb, clone 1HT44H3) (Immunotech, Marseille, France); FITC- and PE-conjugated control mouse IgG1 and IgG2a (Dako, Glostrup, Denmark); goat polyclonal IgG anti-human IL-12 (R&D Systems, Minneapolis, MN, USA); anti-CD28 MoAb (a murine IgG1 MoAb, clone CD28·2) (Immunotech); a murine IgG1 control MoAb, MOPC 21 (Cappel, West Chester, PA, USA); and goat control IgG (Cappel). Recombinant human IL-12 was purchased from PeproTech, Inc. (Rocky Hill, NJ, USA). Recombinant human IFN-α 2a was a gift of Nippon Roche (Tokyo, Japan). A metalloproteinase inhibitor KB8301 was purchased from PharMingen (San Diego, CA, USA). Actinomycin D was purchased from Sigma Chemical Co. (St Louis, MO, USA).

Culture medium
RPMI-1640 medium (Life Technologies, Grand Island, NY, USA) supplemented with penicillin G 100 U/ml, streptomycin 100 μg/ml, L-glutamine 0·3 mg/ml, and 10% FBS (Life Technologies) was used for all cultures.

Cell preparation
Peripheral blood mononuclear cells (PBMC) were obtained from healthy adult volunteers by centrifugation of heparinized venous blood over sodium diatrizoate-Ficoll gradients (Histopaque; Sigma). PBMC were depleted of monocytes and NK cells by incubation with 5 mM L-leucine methyl ester HCl (Sigma) in serum-free RPMI-1640, as described elsewhere [16]. T cells were obtained from the treated cell population by rosetting with neuraminidase-treated sheep red blood cells (SRBC) as described previously [6]. Purified CD4⁺ T cells were prepared further by positive selection with anti-CD4 microbeads and MACS (Miltenyi Biotec, Auburn, CA, USA). The CD4⁺ T cell population obtained in this manner contained <0·1% esterase-positive cells, <0·1% NK cells, <0·1% CD19⁺ cells, and >96% CD4⁺ T cells.

Cell culture techniques for induction of the expression of CD154
Anti-CD3 MoAb, 64·1 was diluted in RPMI-1640 (2 μg/ml), and 50 μl were placed in each well of 96-well flat-bottomed microtitre plates (no. 3596; Costar, Cambridge, MA, USA) and incubated at room temperature for 1 h [17]. Purified CD4⁺ T cells (2 × 10⁵/well) were cultured in wells with immobilized anti-CD3 with or without IFN-α and IL-12. KB8301 was dissolved in dimethylsulphoxide (DMSO), and added to cultures at a final concentration of 10 μM

with 0·01% DMSO to prevent the cleavage of CD154 from the membranes [6]. The cells were incubated for 1–5 days at 37°C in a humidified atmosphere of 5% CO_2 and 95% air.

Immunofluorescence staining of cell surface markers and analysis by flow cytometry
After the incubation, the cells were washed once with phosphate-buffered saline (PBS) containing 2% normal human serum and 0·1% sodium azide (staining buffer). The cells were reacted in suspension by incubating for 30 min at 4°C with saturating concentrations of FITC- or PE-conjugated MoAbs. After the cells were washed twice with staining buffer, they were fixed with 1% paraformaldehyde in PBS pH 7·4 for more than 5 min at room temperature. The cells were analysed using an EPICS XL flow cytometer (Coulter) equipped with an argon-ion laser at 488 nm, as described previously [6]. The percentages of cells staining positively for each MoAb were determined by integration of cells above a specified fluorescence channel, calculated in relation to isotype-matched control MoAb. Density of staining was expressed as the change in mean fluorescence intensity (MFI) for staining with the MoAb of interest calculated by subtracting the MFI of staining with the isotype-matched control MoAb.

RNA isolation and semiquantitative reverse transcription-polymerase chain reaction (RT-PCR)
Total RNA was isolated from cultured cells using the Trizol reagent (Life Technologies) according to the manufacturer's application protocol and quantified spectrophotometrically. cDNA samples were prepared from 1 μg of total RNA using the SuperScript reverse transcriptase preamplification system (Life Technologies) with oligo (dT) primer and subjected to PCR reactions using the following primers: sense, 5′-GGCCATTATGCA CAGGTTGAAT-3′ and antisense, 5′-GGGGAGGGAAGAG ACTGACAAA-3′ for CD154 (387 base pairs (bp)); sense, 5′-AGTTATATCTTGGCTTTTCA-3′ and antisense, 5′-ACCG AATAATTAGTCAGCTT for IFN-γ (356 bp); sense, 5′-GAGG GACTGGTACTGCTTAATCG-3′ and antisense, 5′-CCCTGCC TCACACAGGTTCA-3′ for IL-12Rβ2 chain (516 bp); and sense, 5′-ATGGCCACGGCTGCTTCCAGC-3′ and antisense, 5′-CAGGAGGAGCAATGATCTTGAT-3′ for β-actin (321 bp) as a control. Samples were amplified by AmpliTaq Gold (Perkin Elmer, Emeryville, CA, USA). PCR reactions were carried out as follows: denaturation at 94°C for 30 s; annealing at 58°C (CD154) or 55°C (IFN-γ, IL-12Rβ2 and β-actin) for 30 s; and extension at 72°C for 1 min. After optimal cycles for each PCR reaction, extension was continued at 72°C for additional 10 min. PCR products were analysed by electrophoresis on 1·5% agarose gels and visualized by ethidium bromide staining. Band intensities were then quantified and analysed with NIH image version 1·62. All results were calibrated to the β-actin band intensity amplified from the same cDNA sample. The identity of each PCR product was verified by sequence analysis.

mRNA stability studies
Purified CD4⁺ T cells (2 × 10⁵/well) were cultured in wells with immobilized anti-CD3 with or without IFN-α and IL-12. After 48 h or 96 h of incubation, actinomycin D (10 μg/ml) was added to the cultures. After various times from the addition of actinomycin D, the cells were harvested and total RNA was isolated. cDNA samples were then prepared and subjected to PCR reactions for detection of CD154 and β-actin as described above.

Measurement of IFN-γ and IL-12

IFN-γcontents in the culture supernatants were measured using a solid phase enzyme-linked immunosorbent assay (ELISA) as described previously [6]. IL-12 contents in the supernatants were measured using an ELISA kit, Cytoscreen (BioSource International, Camarillo, CA). The detection limit of the assay was approximately 0·8 pg/ml of IL-12.

Statistical analysis

The results were analysed for statistical significance by paired sample *t*-test.

RESULTS

IFN-α exerts biphasic effects on CD154 expression of immobilized anti-CD3-activated CD4⁺ T cells depending on the state of activation

Figure 1 shows the time kinetics of CD154 protein expression on immobilized anti-CD3-activated CD4⁺ T cells with or without IFN-α and IL-12. CD154 expression was not detected on unstimulated CD4⁺ T cells (data not shown), but was induced after 24 h of stimulation with immobilized anti-CD3. IFN-α significantly suppressed CD154 expression at 24 h of culture irrespective of the presence of IL-12 (Fig. 1b). The effect of IL-12 on the enhancement of CD154 expression was not significant at 24 h of stimulation, as was consistent with previous studies [6]. The expression of CD154 as well as its enhancement by IL-12 was significant at 72 h of stimulation with immobilized anti-CD3, at which time IFN-α still suppressed the expression of CD154, although the suppressive effects appeared to be less marked (Fig. 1b). Between 72 h and 120 h of cultures, a remarkable decline in CD154 protein expression was observed, as was also reported previously [6]. Of note, however, IFN-α significantly enhanced the expression of CD154 on immobilized anti-CD3-stimulated CD4⁺ T cells at 120 h of cultures (Fig. 1b). The enhancement of CD154 expression was dose-dependent between 100 IU/ml and 1 × 10⁵ IU/ml of IFN-α (data not shown). IL-12 also enhanced the expression of CD154 on CD4⁺ T cells at 120 h of cultures. Of note, IFN-α further enhanced
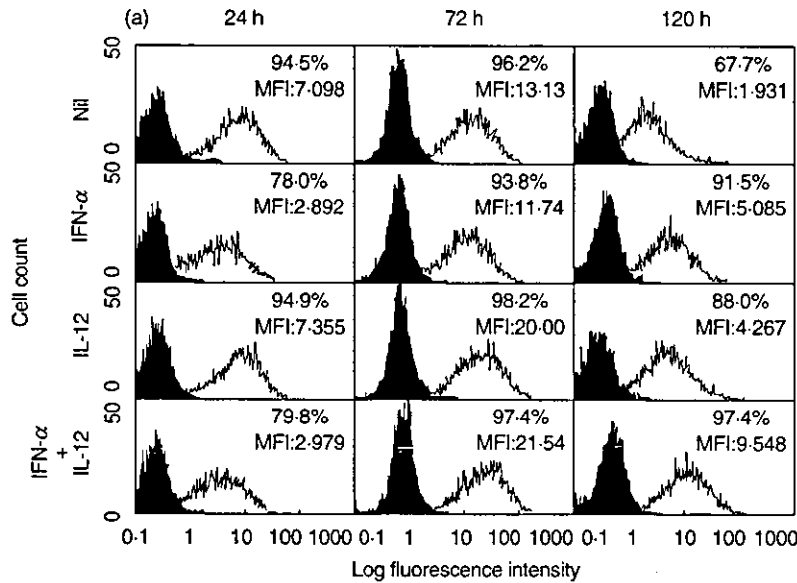
Fig. 1. Time kinetics of CD154 protein expression on immobilized anti-CD3-activated CD4⁺ T cells: effects of IFN-α and IL-12. CD4⁺ T cells (2 × 10⁵/well) were cultured in wells with immobilized anti-CD3 (64·1, 100 ng/well) in the presence of a metalloproteinase inhibitor KB8301 (10 µM) with or without IFN-α (1 × 10⁵ IU/ml) and IL-12 (10 ng/ml). After various periods of incubation, the cells were harvested and stained with FITC-conjugated anti-CD154 (open histogram) MoAb or control MoAb (closed histogram). (a) Percentage of positive and mean fluorescence intensity (MFI) of specific staining for CD154 are indicated. (b) MFI of six independent experiments are indicated. Each line on the graph is representative of the same cell preparation from the same donor. *P < 0·05.
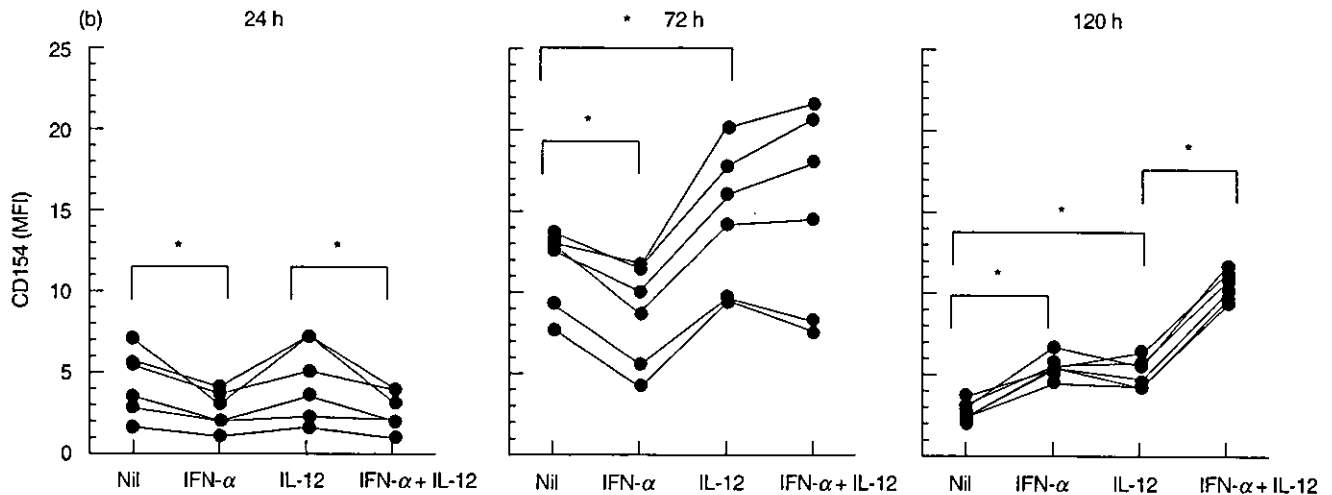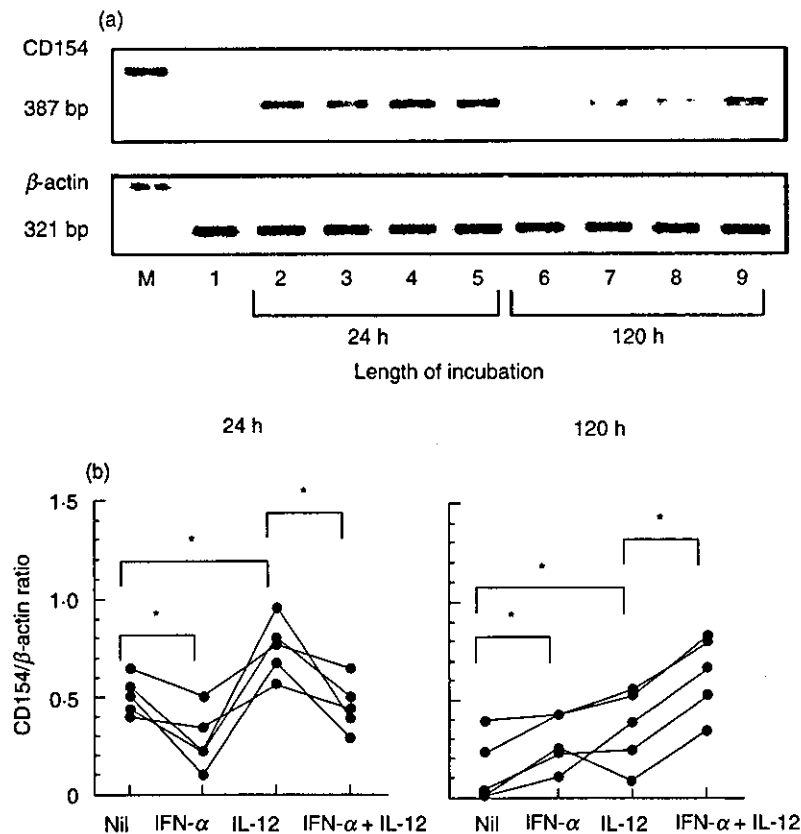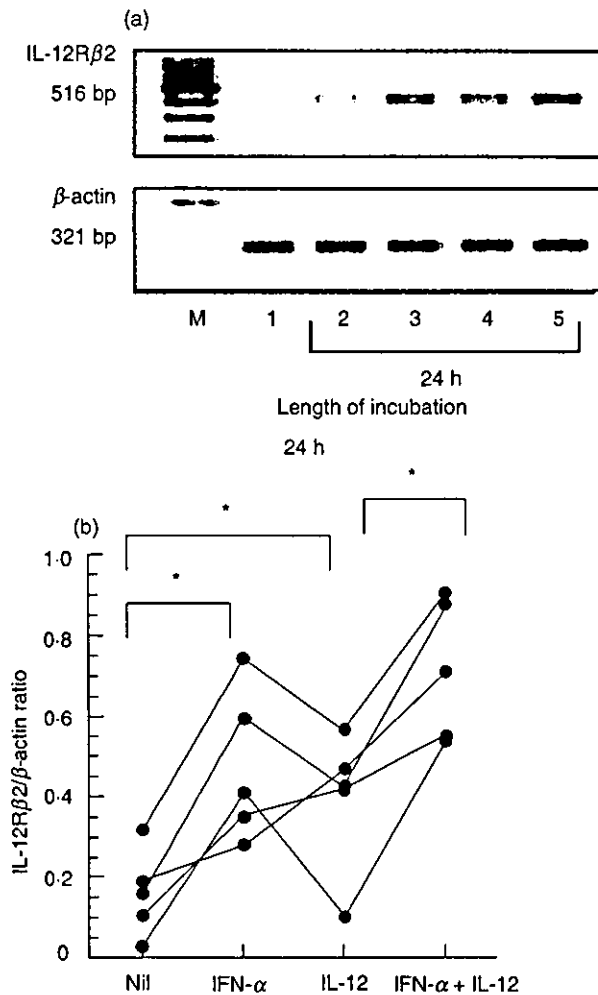
Fig. 2. Time kinetics of CD154 mRNA expression in immobilized anti-CD3-activated CD4⁺ T cells: effects of IFN-α and IL-12. (a) CD4⁺ T cells (2 × 10⁵/well) were cultured in wells with immobilized anti-CD3 (64·1, 100 ng/well) with or without IFN-α (1 × 10⁵ IU/ml) and IL-12 (10 ng/ml). After 24 h or 120 h of incubation, total RNA was isolated and RT-PCR was performed using specific primers for CD154 and β-actin. Lane 1: unstimulated CD4⁺ T cells; lane 2, 6: nil; lane 3, 7: IFN-α; lane 4, 8: IL-12; lane 5, 9: IFN-α + IL-12; M: marker. (b) Densitometric measurement of CD154 mRNA expression. All results were calibrated to the β-actin band intensity. Each line on the graph is representative of the same cell preparation from the same donor. *P < 0·05.

the expression of CD154 on activated CD4⁺ T cells even in the presence of saturating concentrations of IL-12 (10 ng/ml) (Fig. 1b). These results indicate that IFN-α exerts biphasic effects on the expression of CD154 on human CD4⁺ T cells depending on the state of activation irrespective of the presence of IL-12.

The next experiments examined the effects of IFN-α on CD154 mRNA expression in immobilized anti-CD3-activated CD4⁺ T cells, using semiquantitative RT-PCR. As shown in Fig. 2a, CD154 mRNA expression was not detected in unstimulated CD4⁺ T cells. The enhancement of CD154 mRNA expression by IL-12 was observed as early as 24 h, and continued throughout the cultures up to 120 h (Fig. 2b). By contrast, IFN-α down-regulated CD154 mRNA expression significantly irrespective of the presence of IL-12 at 24 h of stimulation (Fig. 2b). However, IFN-α enhanced the expression of CD154 mRNA in anti-CD3-activated CD4⁺ T cells significantly at 120 h of cultures, even in the presence of IL-12 (Fig. 2b). These results indicate that IFN-α also exerts biphasic effects on CD154 mRNA expression, depending on the state of activation of immobilized anti-CD3-stimulated CD4⁺ T cells, whereas IL-12 constantly enhances CD154 mRNA expression in anti-CD3-stimulated CD4⁺ T cells throughout the cultures for as long as 120 h.

IFN-α directly enhances CD154 expression in immobilized anti-CD3-activated CD4⁺ T cells independently of the induction of Th1 responses

It was shown that IL-12Rβ2 subunit, a binding and signal transducing component of IL-12R, is critical for functional IL-12R expression and induction of high affinity IL-12 bindings [18]. As shown in Fig. 3, IFN-α enhanced significantly the expression of IL-12Rβ2 mRNA in immobilized anti-CD3-stimulated CD4⁺ T cells at 24 h of cultures, as is consistent with the previous report [19]. Moreover, the enhancement of IL-12Rβ2 mRNA expression by IFN-α continued throughout the cultures for up to 120 h (data not shown). The data therefore raise the possibility that IFN-α might enhance CD154 expression on anti-CD3-activated CD4⁺ T cells through mechanisms depending on IL-12. However, IL-12 could not be detected in the culture supernatants throughout the cultures of CD4⁺ T cells for as long as 120 h (data not shown). Moreover, neutralizing anti-IL-12 antibody did not influence the IFN-α-mediated enhancement of CD154 expression on CD4⁺ T cells stimulated with immobilized anti-CD3 for 120 h, whereas it abrogated completely the enhancement of the expression of CD154 by IL-12 (Table 1). These results therefore obviate the possibility that the enhancement of CD154 expression of anti-CD3-stimulated CD4⁺ T cells by IFN-α might be mediated by

(a)

IL-12Rβ2

516 bp

β-actin

321 bp

M   1 | 2   3   4   5 |

24 h
Length of incubation

24 h

(b)

IL-12Rβ2/β-actin ratio

1·0
0·8
0·6
0·4
0·2
0

Nil   IFN-α   IL-12   IFN-α + IL-12

Fig. 3. IL-12Rβ2 mRNA expression in immobilized anti-CD3-activated CD4⁺ T cells: effects of IFN-α and IL-12. (a) CD4⁺ T cells (2 × 10⁵/well) were cultured in wells with immobilized anti-CD3 (64·1, 100 ng/well) with or without IFN-α (1 × 10⁵ IU/ml) and IL-12 (10 ng/ml). After 24 h of incubation, total RNA was isolated and RT-PCR was performed using specific primers for IL-12Rβ2 and β-actin. Lane 1: unstimulated CD4⁺ T cells; lane 2: nil; lane 3: IFN-α; lane 4: IL-12; lane 5: IFN-α+IL-12; M: marker. (b) Densitometric measurement of IL-12Rβ2 mRNA expression. All results were calibrated to the β-actin band intensity. Each line on the graph is representative of the same cell preparation from the same donor. *P < 0·05.

the action of IL-12 and thus demonstrate that IFN-α by itself enhances CD154 expression on CD4⁺ T cells independently of IL-12.

As shown in Fig. 4, IFN-α did not enhance IFN-γ production and mRNA expression of anti-CD3-stimulated CD4⁺ T cells, whereas IL-12 significantly enhanced it. Of note, IFN-α did not suppress IFN-γ protein and mRNA expression in CD4⁺ T cells stimulated with anti-CD3 for 24 h. Of more importance, at 120 h of cultures IFN-α significantly enhanced IFN-γ expression only in the presence of exogenous IL-12 (Fig. 4a,c), although IFN-α enhanced CD154 expression even in the absence of exogenous IL-12 (Figs 1b and 2b). These results indicate that the enhancement of IFN-γ protein and mRNA expression of

Table 1. Effect of a neutralizing anti-IL-12 on the enhancement of CD154 expression by IFN-α or IL-12

| | CD154 expression | | | |
| | Control IgG | | Anti-IL-12 | |
Cytokines	Positive (%)	MFI	Positive (%)	MFI
Nil	57·2	1·496	60·2	1·607
IFN-α	81·3	3·114	82·8	3·289
IL-12	73·5	2·357	58·2	1·558
IFN-α + IL-12	90·1	4·893	86·2	3·547

CD4⁺ T cells (2 × 10⁵/well) were cultured in wells with immobilized anti-CD3 (64·1, 100 ng/well) in the presence of a metalloproteinase inhibitor KB8301 (10 μM) with or without IFN-α (1 × 10⁵ IU/ml) and IL-12 (1 ng/ml). Goat polyclonal anti-IL-12 (10 μg/ml) or control goat IgG (10 μg/ml) was added as indicated. After 120 h of incubation, the cells were harvested and stained with FITC-conjugated anti-CD154 MoAb or control MoAb, followed by analysis on flow cytometry. Percentage of positive and mean fluorescence intensity (MFI) of specific staining for CD154 are indicated.

anti-CD3-stimulated CD4⁺ T cells by IFN-α requires the presence of IL-12, whereas the enhancement of CD154 expression by IFN-α does not. In this regard, it is most likely that CD154 expression and IFN-γ production in human CD4⁺ T cells might be regulated differently by IFN-α.

It has been shown that optimal activation of T cells requires signalling through CD28 co-stimulation [20]. It was therefore possible that the lack of enhancement of IFN-γ expression by IFN-α might be due to the absence of CD28 co-stimulation signals. To address this point, experiments were undertaken in which CD4⁺ T cells were stimulated with immobilized anti-CD3 with or without IFN-α and IL-12 for 120 h in the presence of anti-CD28 MoAb or control MoAb. As can be seen in Fig. 5, CD28 co-stimulation enhanced significantly the expression of CD154 mRNA and IFN-γ mRNA, as is consistent with previous reports [20,21]. Of note, even in the presence of CD28 co-stimulation, IFN-α did not enhance IFN-γ mRNA expression, unless IL-12 was supplemented. By contrast, IFN-α further enhanced CD154 mRNA expression in the presence of CD28 co-stimulation irrespective of the presence of IL-12. These results confirm that enhancement of IFN-γ expression in anti-CD3-stimulated CD4⁺ T cells by IFN-α requires the presence of IL-12, but not that of CD28 co-stimulation.

IFN-α and IL-12 do not influence the stability of CD154 mRNA in immobilized anti-CD3-activated CD4⁺ T cells

Final experiments examined whether the enhancement of CD154 mRNA expression in anti-CD3-stimulated CD4⁺ T cells by IFN-α and IL-12 results from an increase in the stability of CD154 mRNA. As shown in Fig. 6, IFN-α and IL-12 had no significant effects on the decay rate of CD154 mRNA in CD4⁺ T cells stimulated with immobilized anti-CD3 for 48 h or for 96 h. The results indicate that IFN-α and IL-12 do not influence the stability of CD154 mRNA in anti-CD3-activated CD4⁺ T cells.
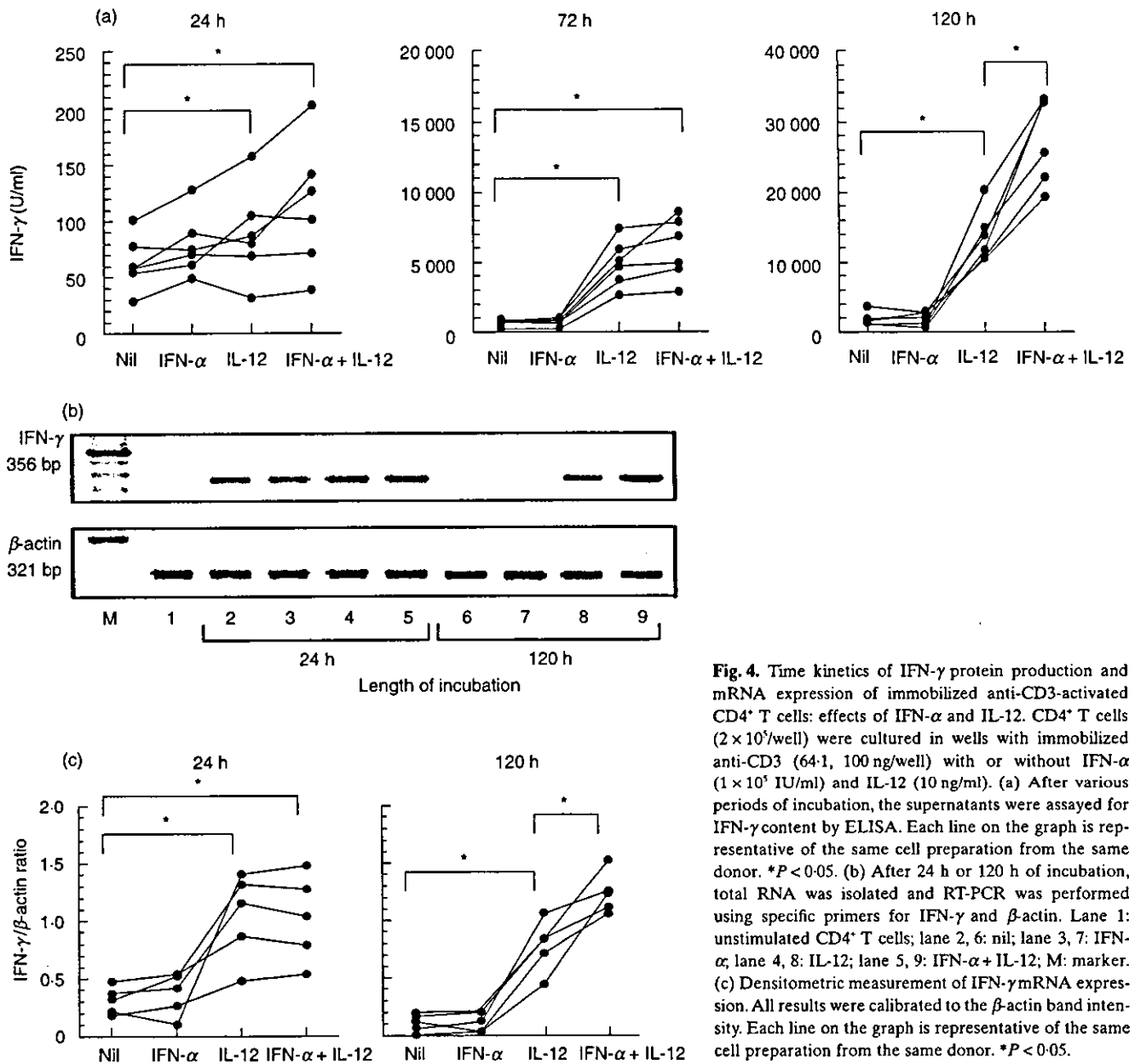
Fig. 4. Time kinetics of IFN-γ protein production and mRNA expression of immobilized anti-CD3-activated CD4⁺ T cells: effects of IFN-α and IL-12. CD4⁺ T cells (2 × 10⁵/well) were cultured in wells with immobilized anti-CD3 (64·1, 100 ng/well) with or without IFN-α (1 × 10⁵ IU/ml) and IL-12 (10 ng/ml). (a) After various periods of incubation, the supernatants were assayed for IFN-γ content by ELISA. Each line on the graph is representative of the same cell preparation from the same donor. *P < 0·05. (b) After 24 h or 120 h of incubation, total RNA was isolated and RT-PCR was performed using specific primers for IFN-γ and β-actin. Lane 1: unstimulated CD4⁺ T cells; lane 2, 6: nil; lane 3, 7: IFN-α; lane 4, 8: IL-12; lane 5, 9: IFN-α + IL-12; M: marker. (c) Densitometric measurement of IFN-γ mRNA expression. All results were calibrated to the β-actin band intensity. Each line on the graph is representative of the same cell preparation from the same donor. *P < 0·05.

DISCUSSION

The current studies investigated in detail the effects of IFN-α on CD154 expression of immobilized anti-CD3-stimulated CD4⁺ T cells. Intriguingly, IFN-α exerted biphasic effects on the expression of CD154, depending on the state of activation of immobilized anti-CD3-stimulated CD4⁺ T cells. Thus, IFN-α suppressed CD154 protein and mRNA expression in the initial phase of activation of CD4⁺ T cells, whereas IFN-α enhanced it at subsequent maturation phase. Because IFN-α suppressed CD25 expression on immobilized anti-CD3-activated CD4⁺ T cells at 24 h of culture (data not shown), it was possible that IFN-α might result in global inhibition of mRNA transcription/translation at the initial activation of CD4⁺ T cells. However, IFN-α enhanced IL-12Rβ2 mRNA expression in anti-CD3-activated CD4⁺ T cells at 24 h of cultures,

as is consistent with previous studies [19]. Moreover, IFN-α did not suppress IFN-γ protein and mRNA expression in the initial activation phase. These results suggest therefore that the suppression of CD154 expression by IFN-α at the initial activation might not a result from global inhibition of mRNA transcription/translation, but be a more specific event, although the precise mechanisms remain to be elucidated.

IFN-α as well as IL-12 enhanced CD154 protein and mRNA expression at 120 h of cultures in CD4⁺ T cells. Of note, IFN-α further enhanced CD154 mRNA expression in activated CD4⁺ T cells even in the presence of saturating concentrations of IL-12, indicating that IFN-α enhances CD154 expression in CD4⁺ T cells through mechanisms different from those of IL-12. It may be argued that IFN-α might enhance CD154 expression through up-regulation of the reactivity to IL-12, as IFN-α
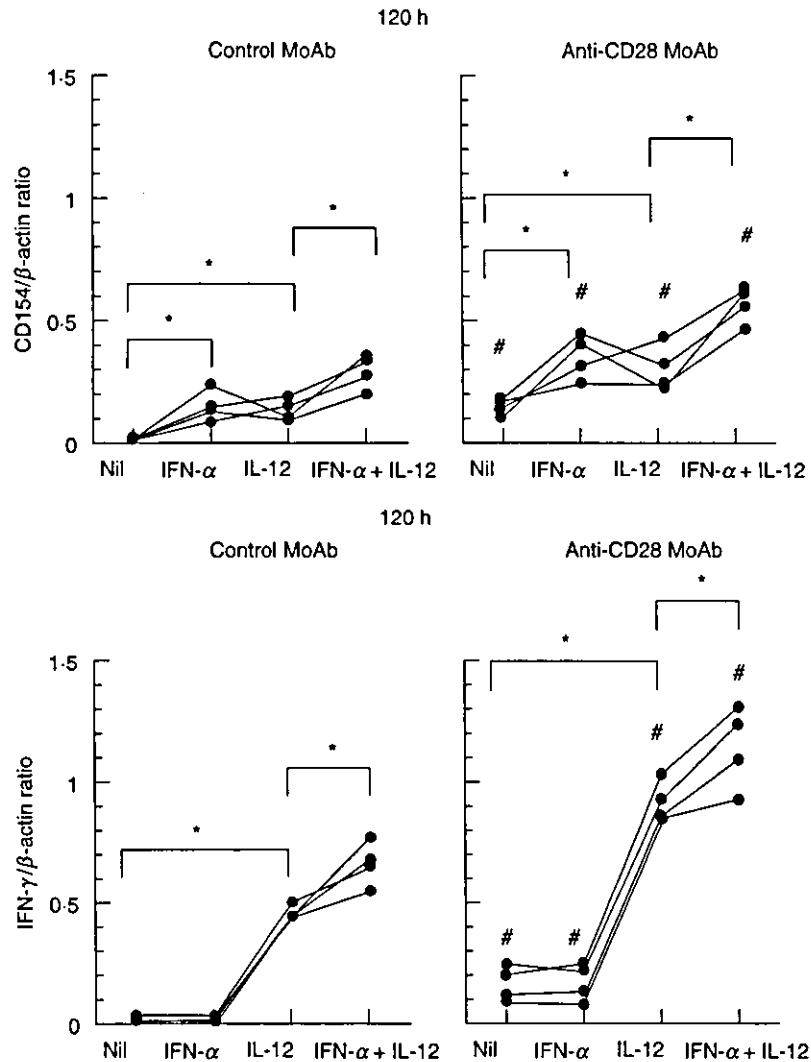
Fig. 5. Effect of IFN-α and IL-12 on the expression of CD154 mRNA and IFN-γmRNA in immobilized anti-CD3-stimulated CD4⁺ T cells: effect of CD28 co-stimulation. CD4⁺ T cells (2 × 10⁵/well) were cultured in wells with immobilized anti-CD3 (64·1, 100 ng/well) with or without IFN-α (1 × 10⁵ IU/ml) and IL-12 (10 ng/ml). Anti-CD28 MoAb or control IgG1 MoAb (4 μg/ml) was added as indicated. After 120 h of incubation, total RNA was isolated and RT-PCR was performed using specific primers for CD154, IFN-γ and β-actin. All results were calibrated to the β-actin band intensity. #$P < 0·05$ compared with cultures with control MoAb in the presence or absence of the same cytokines. Each line on the graph is representative of the same cell preparation from the same donor. *$P < 0·05$.

enhanced the expression of IL-12Rβ2 mRNA in anti-CD3-stimulated CD4⁺ T cells. However, no IL-12 could be detected in the culture supernatants of anti-CD3-stimulated CD4⁺ T cells, reflecting that there was no contamination of monocytes and B cells in the cultures. Moreover, neutralizing anti-IL-12 antibodies did not affect the enhancement of CD154 protein expression by IFN-α, although they totally blocked the enhancing effects of IL-12. The results therefore confirm that IFN-α by itself up-regulates CD154 expression in CD4⁺ T cells independently of IL-12.

Several studies have reported that type 1 IFNs (IFN-α/β) act directly on human, but not mouse, T cells to drive Th1 development, bypassing the need for IL-12-induced signalling [10]. However, the present study demonstrated that IFN-α did not affect IFN-γmRNA and protein expression in CD4⁺ T cells, unless IL-12

was present, suggesting that IFN-α by itself might not be sufficient for the optimal induction of Th1 responses. It should be pointed out that CD4⁺ T cells were activated in the complete absence of accessory cells in the current study, whereas IFN-α induced Th1 responses in the presence of accessory cells in the previous studies [10,19,22]. It has been found that accessory cells provide co-stimulation signals as well as IL-12. It was therefore possible that the inability of IFN-α to enhance IFN-γexpression in anti-CD3-stimulated CD4⁺ T cells might be due to the absence of co-stimulation signals. In the present study, however, IFN-α did not enhance IFN-γ mRNA in anti-CD3-stimulated CD4⁺ T cells even in the presence of CD28 co-stimulation, unless IL-12 was supplemented, confirming that the presence of IL-12 was essential for the up-regulation of IFN-γ expression by IFN-α. It was therefore most probable that IFN-α induced Th1 responses through
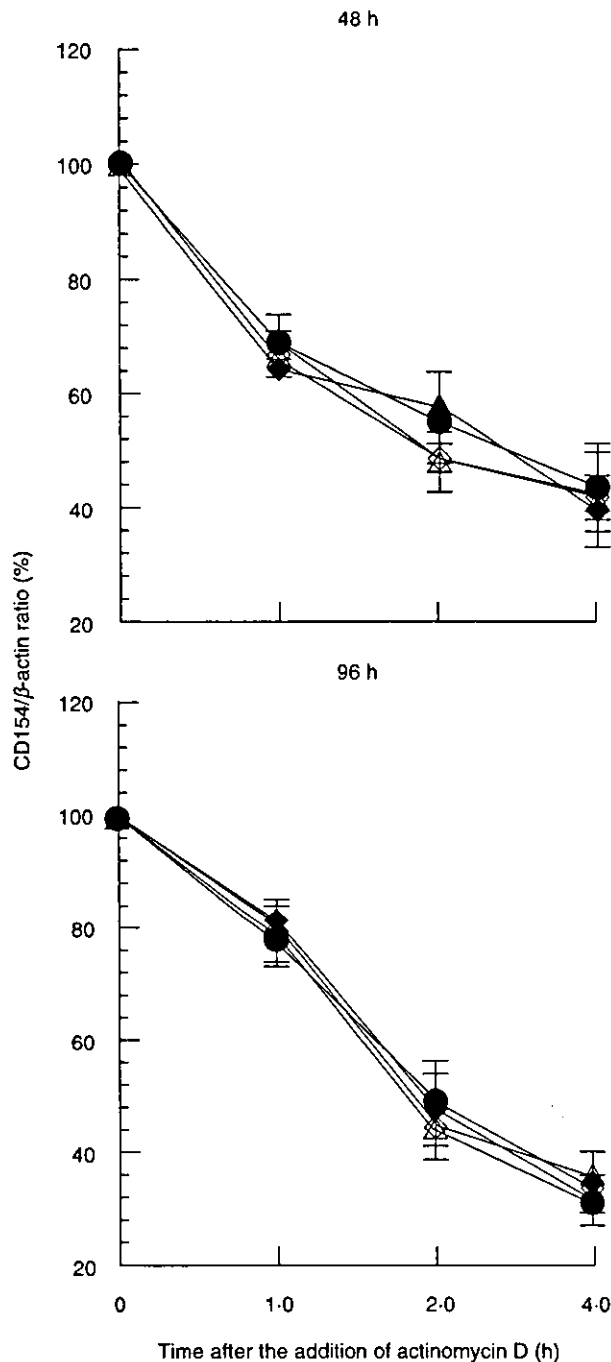
Fig. 6. IFN-α and IL-12 do not influence the stability of CD154 mRNA of CD4⁺ T cells activated with immobilized anti-CD3. CD4⁺ T cells (2 × 10⁵/well) were cultured in wells with immobilized anti-CD3 (64·1, 100 ng/well) with or without IFN-α (1 × 10⁴ IU/ml) and IL-12 (10 ng/ml). After 48 h or 96 h of incubation, actinomycin D (10 μg/ml) was added to the cell cultures. After various times from the addition of actinomycin D, the cells were harvested and total RNA was isolated. Semiquantitative RT-PCR was performed using specific primers for CD154 and β-actin. All results were calibrated to the β-actin band intensity. The data are expressed as the mean ± s.d. (error bars) of three independent experiments. The Y-axis denotes the percent of the CD154/β-actin ratio at the addition of actinomycin D. ◇, Nil; ●, IFN-α; △, IL-12; ◆, IFN-α + IL-12.

up-regulation of the responsiveness to IL-12 secreted from accessory cells in those studies [10,19,22]. Accordingly, a recent study also suggests that IFN-α might enhance IFN-γ production in human T cells by IL-12-dependent mechanisms [23].

Of note, like IL-12, IFN-α has been shown to activate Stat4 [9,10]. However, a recent study has also suggested that activation of Stat4 may not be a sufficient factor for Th1 responses although it is a necessary factor [24]. Moreover, IFN-α can activate Stat4 not only in human Th1, but also in Th2 cells, whereas restimulation of human Th2 lines in the presence of IFN-α does not induce the production of IFN-γ [10]. Collectively, these data suggest the involvement of an important factor other than Stat4 in the expression of IFN-γ mRNA in human T cells. Consistently, recent studies disclosed that mitogen-activated protein kinases (MAPKs) may be involved in a Stat4-independent pathway of IL-12 responsiveness in human T cells [25]. Further studies are required for a complete understanding of the mechanisms of IL-12 signalings that lead to maximal Th1 responses.

A recent study has identified a protein complex which binds to a highly CU-rich portion of the CD154 3′ untranslated region (3′ UTR) and enhances the stability of CD154 mRNA in anti-CD3-activated T cells [26]. Of note, this protein complex was induced in extracts from 24 h and 48 h anti-CD3-activated T cells [26]. As the enhancement of CD154 mRNA by IFN-α and IL-12 was marked later in cultures, it was possible that IFN-α or IL-12 might increase CD154 mRNA expression through up-regulation of such a protein complex. However, neither IFN-α nor IL-12 influenced the stability of CD154 mRNA in 48 h and 96 h anti-CD3-activated CD4⁺ T cells. It is therefore unlikely that these cytokines might increase the expression of such binding proteins. It is suggested, rather, that IFN-α and IL-12 might enhance CD154 mRNA expression in anti-CD3-activated CD4⁺ T cells by up-regulating its transcription, although further studies will be required to confirm this point.

IFN-α is produced by macrophages, DCs and fibroblasts and its production is prominently enhanced during viral and bacterial infection [7]. In this study, the enhancement of CD154 expression on activated CD4⁺ T cells was observed at a dose as little as 100 IU/ml and its expression increased in a dose dependent manner (data not shown). Of note, high serum levels of endogenous IFN-α, which surpasses 2 × 10⁴ IU/ml, are observed in many cases of serious viral infections in humans [27]. It is therefore suggested that IFN-α *in vivo* might contribute to a variety of immune responses through enhancement of CD154 expression in activated CD4⁺ T cells.

REFERENCES

1 Wolf SF, Temple PA, Kobayashi M *et al.* Cloning of cDNA for natural killer cell stimulatory factor, a heterodimeric cytokine with multiple biologic effects on T and natural killer cells. J Immunol 1991; **146**:3074–81.

2 Trinchieri G. Interleukin-12 and its role in the generation of Th1 cells. Immunol Today 1993; **14**:335–8.

3 Manetti R, Parronchi P, Giudizi MG *et al*. Natural killer cell stimulatory factor (interleukin 12 [IL12]) induces T helper type 1 (Th1)-specific immune responses and inhibits the development of IL-4-producing Th cells. J Exp Med 1993; **177**:1199–204.

4 Schmitt E, Hoehn P, Germann T *et al*. Differential effects of interleukin-12 on the development of naive mouse CD4⁺ T cells. Eur J Immunol 1994; **24**:343–7.

5 Peng X, Remacle JE, Kasran A *et al*. IL-12 up-regulates CD40 ligand (CD154) expression on human T cells. J Immunol 1998; **160**:1166–72.

6 Hirohata S. Human Th1 responses driven by IL-12 are associated with enhanced expression of CD40 ligand. Clin Exp Immunol 1999; **115**:78–85.

7 Biron CA, Nguyen KB, Pien GC *et al*. Natural killer cells in antiviral defense: function and regulation by innate cytokines. Annu Rev Immunol 1999; **17**:189–220.

8 Biron CA. Interferons α and β as immune regulators – a new look. Immunity 2001; **14**:661–4.

9 Cho SS, Bacon CM, Sudarshan C *et al*. Activation of Stat4 by IL-12 and IFN-α: evidence for the involvement of ligand-induced tyrosine and serine phosphorylation. J Immunol 1996; **157**:4781–9.

10 Rogge L, D'Ambrosio D, Biffi M *et al*. The role of Stat4 in species-specific regulation of Th cell development by type 1 IFNs. J Immunol 1998; **161**:6567–74.

11 Rönnblom LE, Alm GV, Öberg KE. Possible induction of systemic lupus erythematosus by interferon-α treatment in a patient with a malignant carcinoid tumor. J Intern Med 1990; **227**:207–10.

12 Schilling PJ, Kurzrock R, Kantarjian H *et al*. Development of systemic lupus erythematosus after interferon therapy for chronic myelogenous leukemia. Cancer 1991; **68**:1536–7.

13 Vallin H, Blomberg S, Alm GV *et al*. Patients with systemic lupus erythematosus (SLE) have a circulating inducer of interferon-α (IFN-α) production acting on leucocytes resembling immature dendritic cells. Clin Exp Immunol 1999; **115**:196–202.

14 Desai-Mehta A, Lu L, Ramsey-Goldman R *et al*. Hyperexpression of CD40 ligand by B and T cells in human lupus and its role in pathogenic autoantibody production. J Clin Invest 1996; **97**:2063–73.

15 Koshy M, Berger D, Crow MK. Increased expression of CD40 ligand on systemic lupus erythematosus lymphocytes. J Clin Invest 1996; **98**:826–37.

16 Thiele DL, Kurosaka M, Lipsky PE. Phenotype of the accessory cell necessary for mitogen-stimulated T and B cell responses in human peripheral blood: delineation by its sensitivity to the lysosomotropic agent, L-leucine methyl ester. J Immunol 1983; **131**:2282–90.

17 Geppert TD, Lipsky PE. Accessory cell independent proliferation of human T4 cells stimulated by immobilized monoclonal antibodies to CD3. J Immunol 1987; **138**:1660–6.

18 Presky DH, Yang H, Minetti LJ *et al*. A functional interleukin 12 receptor complex is composed of two β-type cytokine receptor subunits. Proc Natl Acad Sci USA 1996; **93**:14002–7.

19 Rogge L, Barberis-Maino L, Biffi M *et al*. Selective expression of an interleukin-12 receptor component by human T helper 1 cells. J Exp Med 1997; **185**:825–31.

20 Thompson CB, Lindsten T, Ledbetter JA *et al*. CD28 activation pathway regulates the production of multiple T-cell-derived lymphokines/cytokines. Proc Natl Acad Sci USA 1989; **86**:1333–7.

21 Klaus SJ, Pinchuk LM, Ochs HD *et al*. Costimulation through CD28 enhances T cell-dependent B cell activation via CD40–CD40L interaction. J Immunol 1994; **152**:5643–52.

22 Parronchi P, Mohapatra S, Sampognaro S *et al*. Effects of interferon-alpha on cytokine profile, T cell receptor repertoire and peptide reactivity of human allergen-specific T cells. Eur J Immunol 1996; **26**:697–703.

23 Wu CY, Gadina M, Wang K *et al*. Cytokine regulation of IL-12 receptor beta2 expression: differential effects on human T and NK cells. Eur J Immunol 2000; **30**:1364–74.

24 Thierfelder WE, van Deursen JM, Yamamoto K *et al*. Requirement for Stat4 in interleukin-12-mediated responses of natural killer and T cells. Nature 1996; **382**:171–4.

25 Verhagen CE, de Boer T, Smits HH *et al*. Residual type 1 immunity in patients genetically deficient for interleukin 12 receptor β1 (IL-12Rβ1). evidence for an IL-12Rβ1-independent pathway of IL-12 responsiveness in human T cells. J Exp Med 2000; **192**:517–28.

26 Barnhart B, Kosinski PA, Wang Z *et al*. Identification of a complex that binds to the CD154 3′ untranslated region: implications for a role in message stability during T cell activation. J Immunol 2000; **165**:4478–86.

27 Levis SC, Saavedra MC, Ceccoli C *et al*. Correlation between endogenous interferon and the clinical evolution of patients with Argentine hemorrhagic fever. J Interferon Res 1985; **5**:383–9.

Association of Transporter Associated with Antigen Processing Genes with Behçet's Disease in Japanese

K. TAKIZAWA[a,b,*], F. TAKEUCHI[b,†], H. NABETA[b,†], S. HIROHATA[c], A. TAKEUCHI[c], Y. MATSUMURA[d] and K. YAMAMOTO[b]

[a]*Institute of Rheumatology, Tokyo Women's Medical University, 10-22 Kawada-cho, Shinjuku-ku, Tokyo, Japan;* [b]*Department of Medicine and Physical Therapy, Faculty of Medicine, University of Tokyo, 7-3-1 Hongo, Bunkyo-ku, Tokyo, Japan;* [c]*Department of Internal Medicine, Teikyo University School of Medicine, 2-11-1 Kaga, Itabashi-ku, Tokyo 173, Japan;* [d]*Matsumura Clinic and Research Institute for Asthma and Immunological Diseases, 5-52-2 Higashi-Nippori, Arakawa-ku, Tokyo 116, Japan*

Contribution of transporter associated with antigen processing (TAP) genes to the pathogenesis of Behçet's disease (BD) was studied. Restriction fragment length polymorphic analysis of TAP genes was carried out in 46 Japanese patients with BD and 95 healthy subjects. There were no significant differences in allele frequencies of TAP1 and TAP2 genes between whole patients with BD and control population. No significant differences in the frequencies of TAP alleles were observed, when patients of BD with complete type or incomplete type were compared with control population, respectively. An allele frequency of TAP2C was, however, slightly but significantly high in patients with BD who had symptom of erythema nodosum (24.1%) as compared to the control group (11.6%). [$p < 0.05$, $RR = 2.4$]. The allele frequency of TAP2C was slightly high in HLA*B5101 positive patients with BD (28.6%) as compared to HLA*B5101 negative patients (10.9%), but the difference did not reach statistical significance. The absence of genotype TAP2B/C was observed in whole patients group, though it was present in control subjects (14.7%). [$p = 0.003$, $RR = 0.06$]. A genotype frequency of TAP2C/H was high in patients with BD who had symptom of skin lesions (7.5%) as compared to the control group (0.0%). [$p = 0.03$, $RR = 15.4$]. These results suggest the possibility that TAP molecule play some part in formation of skin lesion, such as erythema nodosum in BD in Japanese.

Keywords: Transporter associated with antigen processing (TAP); Behçet's disease; Allele frequency; PCR-RFLP method

INTRODUCTION

Behçet's disease (BD) is a multisystem disorder of unknown origin, characterized by ocular lesions, oral aphthae, skin lesions and genital ulcerations. Although it occurs worldwide, BD is more prevalent in Japanese and in individuals of Mediterranean origin. Therefore, it has been hypothesized that the disease affects predominantly individuals living along the old Silk Route extending from the Orient through Turkey and into the Mediterranean basin.[1] It is well known that in those geographical regions where the disease is most prevalent, HLA-B51 is more common in BD patients than in controls.[2–5] The correlation of it in Japanese patient is, however, not more than 60.0%.[6] Besides, Sun et al.[7] reported increased frequencies of DRw6 and DRw8 antigens in patients with BD as compared with those in control group. In spite of

the presence of these reports, the genetic background of BD is still indistinct.

On the other hand, transporter associated with antigen processing (TAP) proteins whose gene maps within the MHC region are involved in ATP-dependent transport, of peptide fragments that will bind to class I MHC molecules, across ER membranes.[8,9] It is well known that BD show a lymphocytic perivasculitis, and the majority of patients with active BD has increased levels of circulating immune complexes. It has been suggested that TAP gene play as role in the pathogenesis of BD. Powis et al.[10] have reported the polymorphism of TAP1 and TAP2 genes, and Gonza'lez-Escribano et al.[11] have already reported that the frequency of TAP1C is absent and DQB1*0501/TAP2B increased in BD patients.

In this report, 46 Japanese BD patients were studied to clarify the contribution of TAP genes to the disease using

*Corresponding author. Address: Institute of Rheumatology, Tokyo Women's Medical University, 10-22 Kawada-cho, Shinjuku-ku, Tokyo, Japan. Tel.: +81-3-5269-1725. Fax: +81-3-5269-1726. E-mail: takizawa@ior.twmu.ac.jp
†Tel.: 81-3-3815-5411. Fax: 81-3-3815-5954.

the PCR-RFLP (polymerase chain reaction—restriction fragment length polymorphism) method.[12] The prevalence of alleles was calculated in each TAP1 and TAP2 gene, and was compared with control population.

MATERIALS AND METHODS

Patients and Controls

Forty-six Japanese patients with BD and ninety-five unrelated healthy controls were enrolled in this study. These patients were diagnosed according to the standard criteria proposed by the Japan Behçet's Disease Research Committee.[6] They consist of 33 females and 13 males, aged 52.8 ± 12.3 years old. Clinical features are shown in Table I. Peripheral blood was taken from these patients and the normal controls, and genomic DNA was extracted using standard phenol–chloroform extraction procedure.

Genotyping of TAP1 and TAP2 Genes

TAP1 and TAP2 genotyping was performed by the PCR-RFLP method using the specific primers described previously.[13] PCR was carried out by the method of Saiki *et al.*[14] with minor modifications[12] using Taq DNA polymerase (Takara, Tokyo, Japan). PCR cycles consisted of the initial 2 min denaturation at 95 °C; 30 cycles of 1 min denaturation at 95 °C, 1 min annealing at 56 °C, and 1 min extension at 72 °C; followed by 5 min extension at 72 °C. This cycle was performed in a programmable DNA Thermal Cycler (Perkin Elmer Cetus, Norwalk, CT, USA). After amplification, PCR products were digested with each restriction endonuclease. Dimorphic site at TAP1 codon 333 (Val/Ile) and at codon 637 (Asp/Gly) were digested with Sau3AI and AccI, respectively, and TAP2 codon 687 (Gln/Stop) was digested with BfaI. The other three dimorphisms of TAP2 genes were detected by mismatch-PCR-RFLP using AccII (codon 379; Val/Ile), MspI (codon 665; Thr/Ala) and RsaI (codon 565; Thr/Ala). After digestion, the RFLP pattern was determined by 10% polyacrylamide gel electrophoresis.[12] Four possible TAP1 alleles (TAP1A-D) and eight possible TAP2 alleles (TAP2A-H) were determined by a combination of dimorphic sites and were assigned according to nomenclature proposed by Powis *et al.*[10,15]

Genotyping of HLA*B5101

Alleles of HLA*B5101 were analyzed by a PCR-SSOP method. DNA fragments were amplified using the specific primers described previously.[16] PCR cycles consisted of the initial 3 min denaturation at 95 °C; 30 cycles of 30 s denaturation at 95 °C, 30 s annealing at 62 °C, and 1 min extension at 72 °C; followed by 5 min extension at 72 °C. This amplification was performed in a programmable DNA Thermal Cycler (Perkin Elmer Cetus, Norwalk, CT, USA). PCR products (1.5 μl) were applied to a charged

nylon membrane (Amersham, Hybond-N). After nine oligonucleotide probes were labeled with dig-11-ddUTP, respectively, the hybridization was carried out between PCR products and nine probes on the membrane at 42 °C for 30 min. Using alkaline phosphatase labeled anti-dig-antibody, chemiluminescent-detection was performed, as previously described.[17]

Statistical Methods

Allele frequencies were calculated by direct counting. Frequency-comparisons were made by χ^2 analysis with Yates' correction (the level of significance was 0.05) and, when a value below 5 was contained in the 2 × 2 table, Fisher's exact test was used. Relative risk (RR) was calculated by standard Woolf's formula or Haldane's modified formula when "0" was included.

RESULTS

Allele frequencies and genotype frequencies of TAP1 and TAP2 genes in patients with BD were compared with Japanese control population. Allele frequencies of TAP1 and TAP2 are shown in Table II. No significant differences were observed between whole patients with BD and control population in the frequencies of each TAP alleles. In order to clarify whether TAP gene play some part in clinical features in BD, the patients were classified into several groups according to their symptoms, such as ocular lesions, oral aphthae and genital ulcerations. No significant differences in the frequencies of TAP alleles were observed, when patients of BD with complete type or incomplete type were compared with control population, respectively. An allele frequency of TAP2C was slightly but significantly high in patients who had symptom of erythema nodosum (24.1%) as compared to the control group (11.6%). [$p < 0.05$, $RR = 2.4$] The difference of allele frequency of TAP2C did not reach statistical significance, when the patients who had at least one kind of skin lesions, such as erythema nodosum, subcutaneous thrombophlebitis, folliculitis or cutaneous hypersensitivity (18.8%) were compared with control population (11.6%).

A significant higher frequency of HLA-B*5101 was observed in patients with BD (14 of 46 patients; 30.4%)

TABLE I Clinical features of Behçet's disease

	Total (n = 46)	Incomplete (n = 34)	Complete (n = 12)
Female/male	33/13	27/7	6/6
Mean age	52.8 ± 12.3	52.7 ± 14.0	53.1 ± 5.0
Ocular symptoms	27 (58.7%)	15 (44.1%)	12 (100%)
Oral aphthae	43 (93.5%)	31 (91.2%)	12 (100%)
Skin lesions	40 (87.0%)	28 (82.4%)	12 (100%)
Erythema nodosum	29 (63.0%)	20 (58.8%)	9 (75.0%)
Genital ulcer	28 (60.9%)	16 (47.1%)	12 (100%)
Neuro Behçet	9 (19.6%)	7 (20.6%)	2 (16.7%)

TABLE II Allele frequencies of TAP genes in patients with BD and controls [classified by clinical features]

| | Behçet's disease patients | | | | | | | Controls (n = 95) (%) |
| | Total (n = 46) (%) | Complete type (n = 12) (%) | Ocular lesions (n = 27) (%) | Oral aphthae (n = 43) (%) | Genital ulceration (n = 28) (%) | Skin lesions | | |
						Total (n = 40) (%)	Erythema nodosum (n = 29) (%)	
TAP1								
A	87.0	91.7	87.0	88.4	89.3	87.5	89.7	85.3
B	10.9	8.3	11.1	11.6	10.7	11.3	10.3	14.7
C	2.2	0.0	1.9	0.0	0.0	1.3	0.0	0.0
D	0.0	0.0	0.0	0.0	0.0	0.0	0.0	0.0
TAP2								
A	41.3	33.3	38.9	41.9	37.5	38.8	37.9	42.6
B	32.6	33.3	35.2	30.2	32.1	30.0	25.9	34.2
C	16.3	20.8	14.8	17.4	19.6	18.8	24.1*	11.6
D	2.2	8.3	3.7	2.3	3.6	2.5	3.4	1.1
E	4.3	4.2	5.6	4.7	3.6	5.0	3.4	10.0
G	0.0	0.0	0.0	0.0	0.0	0.0	0.0	0.5
H	3.3	0.0	1.9	3.5	3.6	3.8	3.4	0.0

* An allele frequency of TAP2C was slightly but significantly high in patients who had symptom of erythema nodosum as compared to normal subjects. [$p < 0.05$, RR = 2.4].

compared with control population previously reported by Tokunaga et al.[17] (15 of 117 individuals; 12.8%). [$p < 0.025$, RR = 3.0] A significant higher frequency of HLA-B*5101 was observed especially in patients with incomplete type of BD (32.4%) compared with control population (12.8%) [$p < 0.025$, RR = 3.3], but the difference was not statistically significant when the frequency in patients with complete type of BD (25.0%) was compared. An allele frequency of TAP2C was slightly high in HLA*B5101 positive patients with BD (28.6%) as compared to HLA*B5101 negative patients (10.9%). But this difference did not reach statistical significance when evaluated by the p value (Table III).

A phenotype frequency of TAP1C was only 4.3% in the patients with BD and 0% in Japanese normal subjects (Table IV). A phenotype frequency of TAP2H was slightly but significantly high in patients who have symptom of skin lesions (7.5%) as compared to normal subjects (0.0%). [$p = 0.03$, RR = 15.4]. (Data were not shown) This difference was not statistically significant when p value was corrected. ($p_c > 0.05$).

The absence of genotype TAP2B/C was observed in whole patients group, though it was present in control subjects (14.7%). [$p = 0.003$, RR = 0.06].The statistical significance of the difference remained after correction of p value ($p_c = 0.039$). A genotype frequency of TAP2C/H was slightly but significantly high in the patients who had symptom of skin lesions (7.5%) as compared to normal subjects (0.0%). [p = 0.03, RR = 15.4]. The difference was not significant when p value was corrected ($p_c > 0.05$). (Data was not shown)

Besides, we performed HLA class II typing and observed a high frequency of HLA-DR6 in whole patients with BD (34.8%) compared with normal subjects (15.8%). [$p < 0.025$, RR = 2.84](Data were not shown). But the difference was not significant when p value was corrected ($p_c > 0.05$).

DISCUSSION

Susceptibility to BD is influenced by genetic factors mapped within the HLA gene region, and genetic predisposition to the disease is mainly controlled by HLA-B51 or other genes near the HLA-B region. Nevertheless, the involvement of additional genetic factors in pathogenesis of BD is assumed because this association is not complete. Considering the possible function of TAP gene, the polymorphism of TAP gene is interesting candidate of susceptibility.

TABLE III Allele frequencies of TAP1 and TAP2 in patients with BD, [classified according to the existence of HLA-B51]

| | Behçet's disease | | Controls (n = 95) (%) |
	HLA-B*5101 (+) (n = 14) (%)	HLA-B*5101 (−) (n = 32) (%)	
TAP1			
A	82.1	89.1	85.3
B	14.3	9.4	14.7
C	3.6	1.6	0.0
D	0.0	0.0	0.0
TAP2			
A	42.9	40.6	42.6
B	17.9	39.1	34.2
C	28.6†	10.9	11.6
D	0.0	3.1	1.1
E	7.1	3.1	10.0
G	0.0	0.0	0.5
H	3.6	3.1	0.0

† An allele frequency of TAP2C was slightly high in HLA*B5101 positive patients with BD as compared to HLA*B5101 negative patients.